Mem. S.A.It. Vol. 81, 18

Memorie della

The golden age of multifrequency astrophysics

Franco Giovannelli[1] and Lola Sabau-Graziati[2]

[1] INAF - Istituto di Astrofisica Spaziale e Fisica Cosmica, Roma, Area di Ricerca CNR di Tor Vergata, Via Fosso del Cavaliere 100, I 00133 Roma, Italy
e-mail: franco.giovannelli@iasf-roma.inaf.it

[2] INTA - Departamento Programas Espaciales y Ciencias del Espacio, Crta de Ajalvir Km 4, E 28850 Torrejón de Ardóz (Madrid), Spain

Abstract. In occasion of the *Silver Jubilee* of the Frascati Workshop about *Multifrequency Behaviour of High Energy Cosmic Sources* we want to discuss some aspects of the *Multifrequency Astrophysics*. Multifrequency Astrophysics can be considered as a 'new field' of astrophysics born just around the end of 1970-ies – beginning of 1980-ies to which we strongly contributed not only with our own measurements and studies of physical processes spread along the whole electromagnetic spectrum, but mostly with the organization of the Frascati Workshop Series. In this paper we discuss the methodology used in astrophysics for collecting data coming from multifrequency observations of cosmic sources – obtained in different ways – and the relative models developed through theoretical study of physical processes governing their behaviour. Several examples about X-ray binaries, cataclysmic variables, T Tauri stars, relativistic jets from different classes of sources, gamma-ray bursts, and few words about Standard Big Bang Cosmology and experimental proofs fitting the theory will be discussed. We will briefly discuss also the prospects of the multifrequency astrophysics which is now in its golden age without any pretension of completness.

Key words. Experimental Astrophysics: multifrequency – Theoretical Astrophysics: multifrequency – X-ray Binaries – Cataclysmic Variables – T Tauri Stars – Jets – Gamma-ray Bursts – Cosmology: Big Bang

1. Introduction

Multifrequency observations are a typical collaboration task between different 'kinds' of astronomers The idea of collecting them together was born some time ago during the historical first 'Frascati 1984 Workshop' on Multifrequency Behaviour of Galactic Accreting Sources (Giovannelli, 1985). Traditional observations with a single instrument, sensitive to a given frequency, give only partial knowledge of the observed object. To obtain a complete picture of the object, we need either its multifrequency imaging either its multifrequency spectrum. Figure 1 shows clearly the necessity of measuring the multifrequency spectrum of the 197 ms pulsar (Nel & De Jager, 1994). Indeed, if we take only the soft X-ray spectrum derived by EINSTEIN's data (Cheng & Helfand, 1983) and we try to extrapolate this power–law spectrum to higher energies, we completely misunderstand the behaviour of the pulsar, being its spectrum at higher energies derived by GRO-EGRET's

Send offprint requests to: F. Giovannelli

data completely different (Fierro et al., 1993); and also the extrapolation of EGRET's data to lower energies would completely fails the fit.

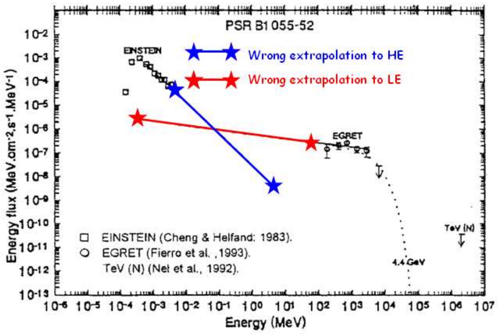

Fig. 1. Energy spectrum of the radio pulsar PSRB 1055-52 (Reprinted with permission from Nel, H.I. & de Jager, O.C., AIP Conf. Proc., Vol. 304, Page 91 (1994). © 1994, American Institute of Physics). Wrong extrapolations to low energies (red) and to high energies (blue) are superimposed.

Among celestial objects, high energy (HE) cosmic sources are especially interesting from the point of view of multifrequency observations. Collapsed objects, close binaries, supernova remnants (SNRs), pre-main-sequence stars, active galactic nuclei (AGNs), gamma–ray bursts (GRBs) experience particularly violent phenomena of high complexity, and emit radiation over the whole electromagnetic spectrum. Among the HE cosmic sources, X-ray binaries constitute the most rich laboratory for multifrequency observations: they are a cauldron of different physical processes which occur at different frequencies and in different time scales (e.g. Giovannelli & Sabau-Graziati, 2001).

The experiments outside the atmosphere started in 1946, soon after the end of the second world war, when the Naval Research Laboratory (NRL) launched a V2 rocket with a payload which observed the Sun's UV spectrum.

Since that time many space experiments were prepared and several fundamental results were reached. In our opinion the actual beginning of the Space Era for studying the Universe is the year 1962. An X-ray experiment — prepared by Giacconi, Gursky, Paolini & Rossi — launched on board an Aerobee rocket discovered a strong X-ray emission from an extrasolar object, namely Sco X-1 (Giacconi et al., 1962). After this first historical experiment many others were launched on board rockets and later balloons and satellites. These experiments brought to our knowledge a really and until that time unknown, of an X-ray sky which started to give experimental proofs of the first theories of Baade & Zwicky (1934) about the possible existence of neutron stars.

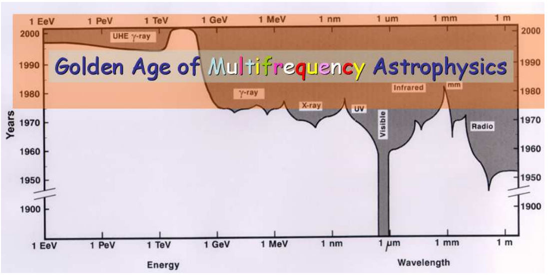

Fig. 2. Amount of astronomical data acquired across the electromagnetic spectrum during last century (after Giovannelli & Sabau-Graziati, 2004, updated from Lena, 1988).

Undoubtedly the advent of spacecrafts gave a strong impulse to astronomy; starting roughly from middle '70ies almost all the electromagnetic spectrum was continuously surveyed by the many space experiments.

Thanks to the improving technologies, experiments in different energy ranges, such as Gamma, UV, Optical and IR, were launched on board rockets, balloons and satellites. A large amount of excellent-quality data coming from those space experiments rendered the data, acquired during many centuries from the ground, only a small fraction of the total now available. Then, the **GOLDEN AGE of Multifrequency Astrophysics** began.

The results from the whole set of space experiments improved the knowledge of the entire structure of the Universe and the *monochromatic optical old sky* became a *polychromatic new sky*, containing all the information necessary in understanding the physics governing the Universe itself. Figure 2 shows the amount of astronomical data acquired across the electromagnetic spectrum during last century (e.g. Giovannelli & Sabau-Graziati, 2004, updated from Lena, 1988).

Thus photonic astrophysics appears to be the most promising and suitable probe in sounding the Universe.

Let we discuss briefly what we can learn from multifrequency observations of HE cosmic sources dividing the electromagnetic spectrum in different energy ranges, which are essentially depending on the techniques used for detecting the emissions from cosmic sources:

- μ–wave, sub–millimetric, millimetric energy regions: information about cosmic microwave background (CMB), molecules, dust grains in stellar forming regions, and pre–main sequence stars (PMSSs).
- radio energy region: information about free–free emissions from winds, and mass loss rates and circumstellar geometries.
- Infrared (IR) energy region: information about free–free emissions from winds, and mass loss rates; dust emissions and dust properties; emission lines from gases and mass loss rates and extinction.
- optical energy region: information about the continuum emissions of stars and galaxies and then effective temperatures and bolometric luminosities; emission lines from gases and mass loss rates; photospheric stellar profiles and then rotational velocities and no–radial pulsations; linear and circular polarizations and then knowledge of winds and circustellar geometries.
- Ultraviolet (UV) energy region: information about the continuum emissions and then effective temperatures and bolometric luminosities; wind profiles via resonance lines, such as CIV and SiIV, and then wind structuers, terminal velocities of winds, variabilities; photospheric stellar profiles, such as i.e. HeII, and then rotational velocities and no–radial pulsations.
- X–ray energy region: information about shock emissions and then wind structures and variabilities; coronal emissions and then information about the binary companion; accretion processes and the physics of accretion disks.
- γ–ray region: information about HE nuclear reactions, HE phenomena, such as nuclei de-excitations, meson decay, matter-antimatter annihilation, point–like sources, GRBs.

2. Multifrequency astrophysics

Multifrequency astrophysics develops into *Experimental multifrequency astrophysics* and *Theoretical multifrequency astrophysics*. We will discuss both items through several examples coming from our direct experience. Our purpose is to render enough clear the importance of multifrequency astrophysics as new technique of investigation and methodology for its development. It is obvious that both experimental and theoretical multifrequency astrophysics converge to a better understanding of the physics governing our Universe (e.g. Giovannelli & Sabau–Graziati, 2004).

2.1. Experimental multifrequency astrophysics

Experimental multifrequency astrophysics can be developed as follows: a) Simultaneous Multifrequency Observations; b) Coordinated Multifrequency Observations; c) Data base and/or Literature observations; d) Multifrequency Observations (not necessarily simultaneous); e) Multisites Observations.

2.1.1. Simultaneous multifrequency observations

Simultaneous multifrequency observations can be performed with different experiments and/or facilities in different energy ranges (i.e. when it is necessary to get the total energy distribution of a source, or to search for energy dependent variations). For instance, the study of PMSSs is of great interest as it provides crucial information on the role of magnetic fields, angular momenta, accretion of matter, and mass–loss processes, as well as indirect information on the formation processes of the Sun and solar system. In this framework, very important results were obtained for the classical T Tauri star RU Lupi which was a special target for coordinated, sometimes simultaneous multifrequency observations (e.g. Giovannelli et al., 1990a; 1995). These results allowed to model the multifrequency behaviour of RU Lupi (Lamzin et al., 1996). Among the many results obtained in the long campaign of coordinated observations, spread between 1983 and 1988, the total energy distribution in quiescence and during Flare-like Events (FLEs) obtained simultaneously from UV to IR in five occasions is the highlight result. This allowed to determine the energy budget during FLEs. Figure 3 shows the five simultaneous observations of RU Lupi, as discussed by Giovannelli (1994) and Giovannelli et al. (1995).

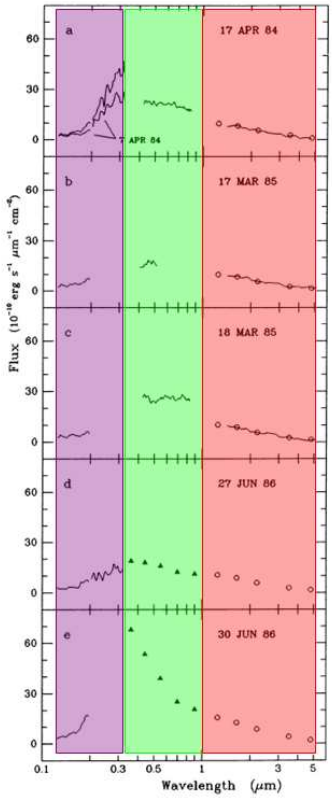

Fig. 3. Total energy distributions of RU Lupi, simultanously obtained in UV (violet), optical (green), and IR (red) regions (after Giovannelli et al., 1995).

2.1.2. Coordinated multifrequency observations

Coordinated observations are very useful either when it is not possible for any reasons to perform simultaneous observations or when a certain phenomenon is expected to appear in particular different moments dependent on the energy (i.e. in hard X-ray transient sources, X-ray outbursts appear delayed with respect to strong optical activity). We can discuss, as example, the cases of the X–ray/Be system A0535+26/HDE245770, jet–sources, and gamma–ray bursts (GRBs).

2.1.2.1. A0535+26/HDE245770 system

The X-ray pulsar A0535+26 was discovered by the Ariel V satellite on April 13, 1975 (Rosenberg et al., 1975). It reached an intensity of about 2 Crab and the signal was pulsed at about 104 s. For a general review see the paper by Giovannelli & Sabau-Graziati (1992). Our group started a methodical observations of a star within the error box of the X-ray source, named HDE 245770, which was the unique star with H_α line in emission. For this reason, indeed this star was suspected to be the optical counterpart of the X-ray pulsar (e.g. Liller, 1975, Murdin, 1975, Soderblom, 1976, Giangrande et al., 1977). However, a spectrophotometric survey of the stars within the error box of the X-ray pulsar up to the 23rd magnitude did not show any pulsation at 104 s, like in the X-ray energy range; only an upper limit of 0.0002 magnitudes. So the open problems were both the identification of the real optical counterpart and its spectral classification. During 1977-78 A0535+26 was observed by the SAS 3 satellite and the position was defined as better as 20 arcsec; this small error box contained the HDE245770 early type star. Then the identification of HDE245770 as the optical counterpart of the X-ray pulsar A0535+26 was virtually certain (Li et al., 1979), but not yet definitively proved.

Our efforts in solving both the identification of the real optical counterpart (Bartolini

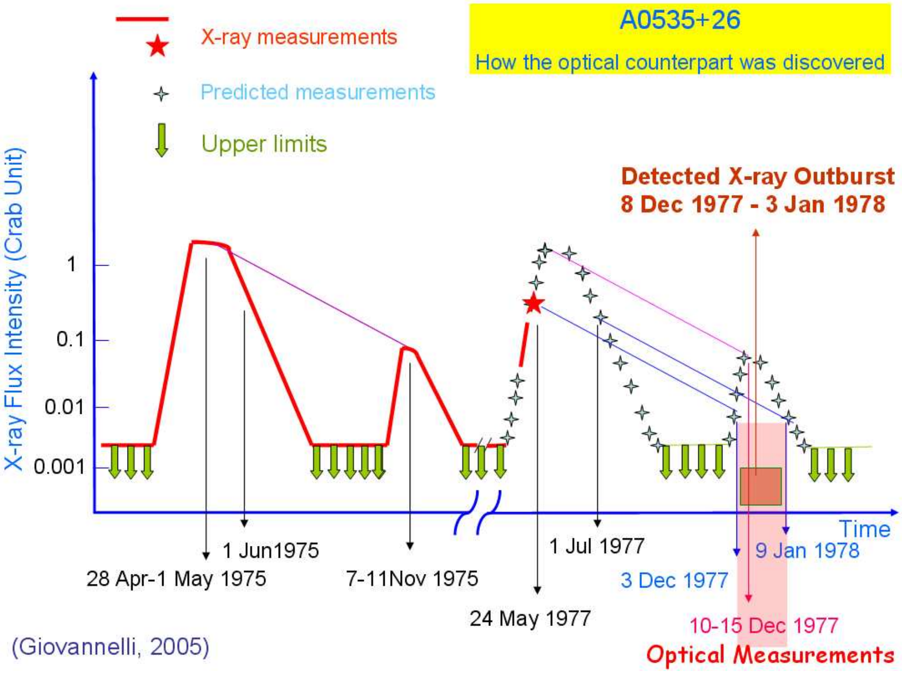

Fig. 4. How the association of the optical counterpart of A0535+26 was found (Giovannelli, 2005).

et al., 1978) and its spectral classification were rewarded (Giangrande et al., 1977; Giangrande et al., 1980). Indeed, an optical outburst of HDE245770 correlated with the December 1977 X-ray outburst of A0535+26 gave the first direct proof of the association of the two objects. Our optical measurements during December 1977 were not obtained by chance, but thanks to a prediction made by Franco Giovannelli (FG) under the hypothesis that the few X-ray outbursts detected were roughly periodic. This is clearly reported in Figure 4 (Giovannelli, 2005), where the first two detected X-ray outbursts are reported in red as well as the few measurements during the ”rise” of the third outburst. And here there was FG’s intuition: since the slope of the rise was similar to that of the first outburst, FG made the hypothesis that a similar outburst would have occurred (the third) and then a fourth one, similar to the second, would have occurred simply with a same delay of the second with respect to the first outburst. In this way FG predicted a possible X-ray outburst of the A0535+26 pulsar in the period ranging from December 3, 1977 to January 9, 1978, with a maximum around December 10-15. On December 17, we measured a decay from an outburst of HDE245770. The X-ray outburst was announced a few days later by Chartres and Li (1977) thanks to SAS 3 measurements (maximum in 2-10 KeV on December 23.5) , and much later the entire 1977 December X-ray outburst at different energies was reconstructed (see Table 1 of the review by Giovannelli & Sabau-Graziati, 1992). The outburst started on December 8, 1977 and was still strong on January 3, 1978. After this date no measurements are available. Then, the ”hazardous” FG’s prediction was awarded by the first direct evidence about the association of the O9.7IIIe star HDE245770 with the X-ray pulsar A0535+26 (see the IAU Circular N. 3167 by Bartolini et al., 1978).

Soon after the definite association of HDE 245770 — later nicknamed Flavia’ star

(Giovannelli & Sabau–Graziati, 1992) — as companion of A0535+26 X–ray pulsar, our group provided its classification as O9.7 IIIe star (Giangrande et al., 1980), its distance to Earth (1.8 ± 0.6 kpc, mass and radius ($M_\star$ = 15 $M_\odot$, $R_\star$ = 14 $R_\odot$). This classification, after 29 years, still resists to the many tentative of 'new' classification.

With the advent of the IUE satellite, FG's group started a long series of UV observations of HDE245770/A0535+26 system, as well as the X-ray measurements with the Soviet ASTRON satellite, and optical and IR observations, with numerous programs having FG as PI. The goal of these programs were the knowledge of the morphology of the system, the total energy distribution, the interactions between the neutron star and the Be star, the problem of the mass loss from the Be star and the accretion of matter onto the neutron star. When the knowledge of the system was growing, we successfully attempted with an "heroic IUE program" to follow the system during an entire X-ray outburst predicted by ourselves on the base of their repetition with the orbital period (∼ 111 days) found in X-ray range by Priedhorsky & Terrell (1983) and in optical by Guarnieri et al. (1985).

The delay between the optical and X-ray outbursts of about one week was not clear at that time. But later increasing the knowledge of this system, such a delay appeared natural; it is due to the transit time of the matter ejected from the Be star (∼ 300 Km s^{-1}) onto the neutron star separated by ∼ 1.34 AU.

As example of coordinated observations, it is interesting to look at the Figure 5, where the energy distribution from UV to IR is reported (de Loore et al., 1984). A clear IR excess is present. From these measurements the luminosity and effective temperature were derived ($\log L/L_\odot = 4.87$; $\log T_{\rm eff} = 4.42$).

Multifrequency no–simultaneos observations of A0535+26/HDE245770 system allowed to solve the problems of mass loss rate, spin up of neutron star, identification of different X–ray outbursts triggered by different states of optical companion (e.g. Giovannelli & Sabau–Graziati, 1992), the identification of the presence of a temporary accretion disk around

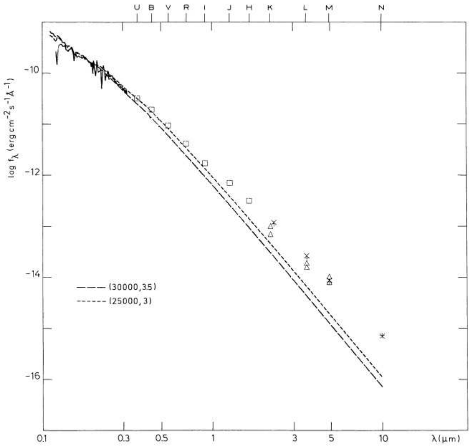

Fig. 5. Total energy distribution of Flavia' star, optical counterpart of A0535+26 X–ray pulsar (Credit: de Loore et al., A&A, 141, 279, 1984, reproduced with permission © ESO).

the neutron star at periastron (Giovannelli et al., 2007), and to find the cyclotron line at ∼ 110 keV, together with cyclotron lines of many other X–ray pulsars (Orlandini & dal Fiume, 2001). Coburn et al. (2002) derived the magnetic field intensity of 10 X–ray pulsars which is ranging from 1.3 to 4.8 $\times 10^{12}$ G.

From UV and optical measurements we detected interstellar, symmetrical and asymmetrical lines and the energy distribution, which was used to find the reddening of the system as E(B-V) = 0.75 ± 0.05 mag, by filling the 2200 Å bump (Giovannelli et al., 1980). From the rotational broadening of He II (1640 Å) symmetrical line, Giovannelli et al. (1982) derived the rotational velocity $v \sin i = 230 \pm 45$ km s^{-1}, in agreement with that derived from He I (4471 Å) by Giangrande et al. (1980), and from asymmetrical resonance lines of Si IV and C IV the terminal velocity of the stellar wind as $v_\infty \sim 630$ km s^{-1}, and mass loss rate of $\dot{M} \sim 10^{-8}$ $M_\odot$ yr^{-1} during a quiescence state of the X–ray source. During a strong outburst the mass loss rate was derived as $\dot{M} \sim 7.7 \times 10^{-7}$ $M_\odot$ yr^{-1} (de Martino et al., 1989). Giovannelli et al. (2007) derived the inclination angle i = 37° ± 2°, which gives the corresponding equatorial rotational velocity of the O9.7IIIe star as 382 ± 40 km s^{-1}.

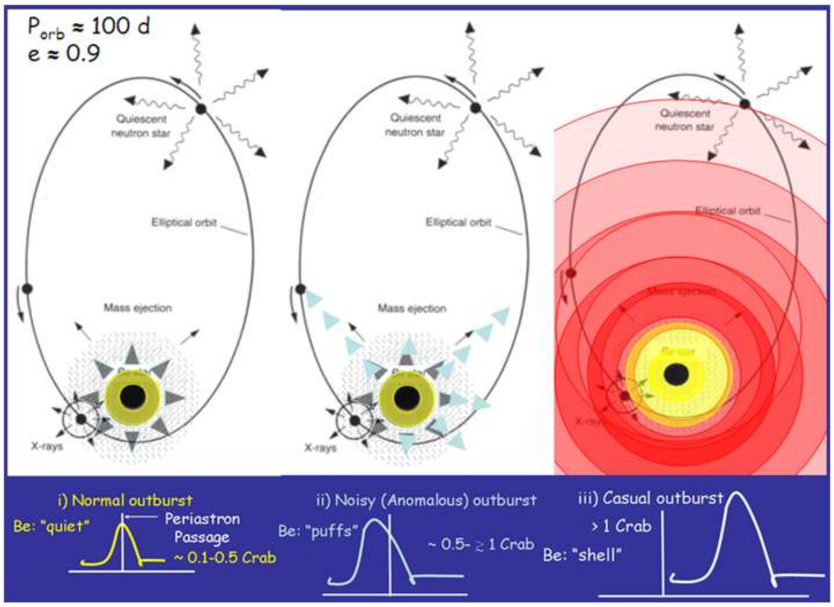

Fig. 6. Sketch of three kinds of X-ray outbursts of an X-ray/Be system with high eccentricity, and long orbital period, induced by the interactions between the Be star, in different states of activity, and the neutron star (after Giovannelli & Sabau-Graziati (2008).

Analysis of a long series of X-ray outbursts as well as the behaviour of the O9.7IIIe star for the A 0535+26/HDE245770 system (Giovannelli & Sabau-Graziati, 1992) allowed to understand the reasons of different kinds of outbursts in the X-ray/Be system class. Figure 6 shows the three kinds of X-ray outburst, namely *normal*, *anomalous (or noisy)*, and *casual* for a generic X-ray/Be system with e $\approx$ 0.9 and $P_{orb} \approx 100$ d. Normal outburst occurs at the periastron passage of the neutron star when the Be star is 'quiescent': only the 'quiescent' stellar wind is escaping from the Be star. Anomalous outburst occurs around — not necessarily at — the periastron passage of the neutron star when the Be star is experiencing an emission of 'puffs' of material superimposed to 'quiescent' stellar wind. Casual outburst occurs in principle at any orbital phase when the Be star expels a shell (repetition time of order thousand days). The intensity of X-ray outbursts is $\sim$ 0.1–0.5, $\sim$ 0.5–1, and $>$ 1 Crab for normal, anomalous and casual outbursts, respectively (Giovannelli & Sabau-Graziati, 2008).

From the secular history of the spin period of the pulsar, Giovannelli et al. (1984) derived $\dot{P}/P = -6.8 \times 10^{-4}$ yr^{-1}, as shown in Figure 7 (Giovannelli et al., 1990b). Thanks to the knowledge of the spin period history of the X-ray pulsar, which experiences periods of spin-up followed by spin-down, Giovannelli & Ziolkowski (1990) discussed the possibility of a temporary formation of an accretion disk around the neutron star at the periastron passage. This work is important since among other results touches the problem of the possible equilibrium period of X-ray pulsars reached now and then with the consequent switched off of the X-ray emission and again switched on. We have measured with the ASTRON satellite the X-ray emission from A0535+26 and in a couple times we did not detect any significant emission although it was expected because of the passage of the neutron star at the periastron (Giovannelli et al., 1985, 1986a). After those two lacks of outbursts, the pulsar flared

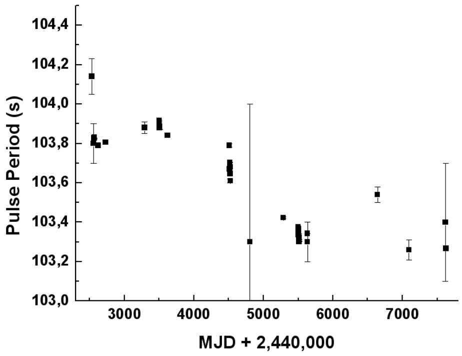

Fig. 7. 1975–1989 spin–up history of the X–ray pulsar A0535+26 (after Giovannelli et al., 1990b).

up again from October 28 to November 1, 1986 (Giovannelli et al., 1986b) and on February 20, 1987 (Giovannelli et al., 1987).

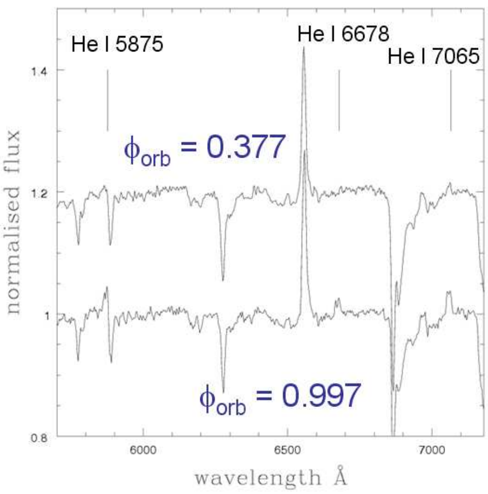

Fig. 8. Spectra of HDE 245770 taken on October 12 (lower) and November 24, 1999 (upper). The flux of the upper spectrum is multiplied by 1.2 for a better representation (after Giovannelli et al., 2007).

It is worthwhile to note that a few years later, Finger, Wilson & Harmon (1996) have found the evidence of the formation of a temporary accretion disk around the neutron star A0535+26 during the February-March 1994 X–ray outburst. Giovannelli et al. (2007) found experimental evidence of the presence of a temporary accretion disk around the neutron star by using He I emission lines. At the periastron He I lines show doubling, while out of the periastron the doubling is absent, as shown in Figure 8. The doubling width is associated with the velocity of material in the outer edge of the accretion disk (Smak, 1969, 1981; Huang, 1972), then it was possible to derive the dimensions of the accretion disk: its radius can range from $(5.9 \pm 0.1) \times 10^{10}$ cm to $(2.1 \pm 0.1) \times 10^{11}$ cm.

2.1.2.2. Relativistic Jets

Relativistic jets have been found in numerous galactic and extragalactic cosmic sources at different energy bands. The emitted spectra of jets are strongly dependent on the angle formed by the beam axis and the line of sight, and obviously by the Lorentz factor of the particles (e.g. Bednarek et al., 1990 and the references therein). Observations of jet sources at different frequencies can provide new inputs for the comprehension of such extremely efficient carriers of energy, like for the cosmological GRBs. The discovered analogy among μ–QSOs, QSOs, and GRBs is fundamental for studying the common physics governing these different classes of objects via μ–QSOs, which are galactic, and then apparently brighter and with all processes occurring in time scales accessible by our experiments (e.g. Chaty, 1998).

Chaty (2007) remarked the importance of multifrequency observations of jet sources by means of the measurements of GRS 1915+105, taken in 1997. The link between accretion and ejection is visible examining Figure 9. We can see the disappearance of the internal part of the accretion disk, shown by a decrease in the X–ray flux, followed by an ejection of relativistic plasma clouds, corresponding to an oscillation in the near–infrared (NIR) and then in the radio, the clouds becoming progressively optically thin.

Paredes et al. (2006) discussed the spectral energy distribution (SED) of the μ–QSO LS 5039 from radio to Tev energies, by using data coming from different experiments, as shown in Figure 10 (Paredes, Bosh-Ramon & Romero, 2006). The effects of the absorption are evident in the SED, where there is a min-

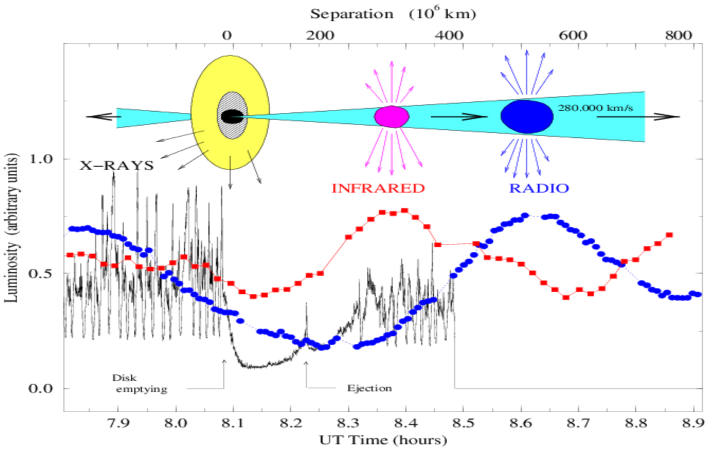

Fig. 9. Observation of the link between accretion and ejection. X-ray, NIR and radio light curves of GRS 1915+105 during the 1997 September 9 multifrequency observation campaign. The disappearance of the internal part of the accretion disc (decrease in the X-ray flux) is followed by an ejection of relativistic plasma clouds (oscillation in the NIR and radio) (Chaty, 2007 and the references therein) (reproduced with kind permission of Società Italiana di Fisica).

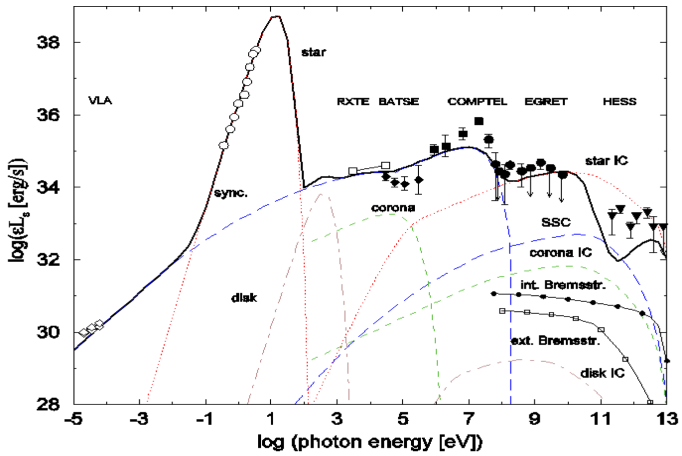

Fig. 10. Spectral Energy Distribution of the μ–QSO LS 5039 (Credit: Paredes, Bosch-Ramon & Romero, A&A, 451, 259, 2006, reproduced with permission © ESO).

imum around few 100 GeV. Figure 11 shows the model derived for such a μ–QSO (Paredes, 2006).

LS 5039 has recently been detected as a source of VHE γ-rays. This detection, that confirms the previously proposed association of LS 5039 with the EGRET source 3EG J1824.1514, makes of LS 5039 a special system with observational data covering nearly all the electromagnetic spectrum.

Dermer et al. (2009) suggest that ultra-high energy cosmic rays (UHECRs) could come from black hole jets of radio galaxies. Spectral signatures associated with UHECR

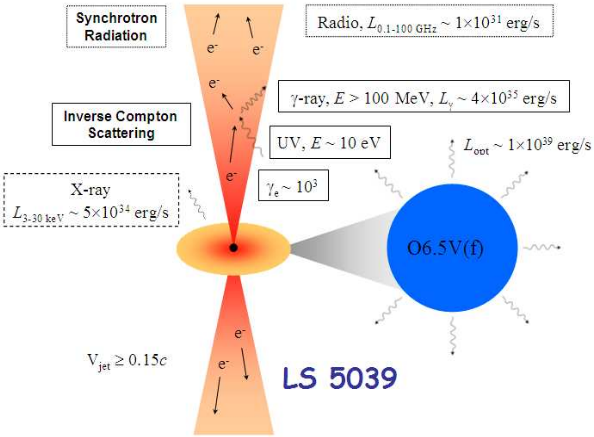

Fig. 11. Sketch of the model of the μ–QSO LS 5039 for explaining its SED (courtesy of Paredes, 2006).

hadron acceleration in studies of radio galaxies and blazars with FERMI observatory and ground-based γ-ray observatories can provide evidence for cosmic-ray particle acceleration in black hole plasma jets. Also in this case, γ-ray multifrequency observations (MeV–GeV–TeV) together with observations of PeV neutrinos could confirm whether black-hole jets in radio galaxies accelerate the UHECRs.

2.1.2.2. Gamma–ray bursts

Gamma–ray bursts (GRBs) are sudden events of a few seconds duration, different from each other both in intensity and duration. The same GRB manifests in different energy ranges with some delays (e.g. Nicastro et al., 2001).

Since their discovery in 1967 — thanks to the four VELA spacecraft, originally designed for verifying whether the Soviet Union abided the 1963 Limited Nuclear Test Ban Treaty — when 16 strong events were detected (Klebesadel, Strong & Olson, 1973), GRBs have remained a puzzle for the community of high energy astrophysicists. For this reason the problem of GRBs originated hundreds of papers most of them devoted to their physical interpretation. Mazets & Golenetskii (1988) reviewed on observations of GRBs until roughly the end of 1980s.

After the launch of the RXTE and BeppoSAX it has been possible to perform multifrequency observations of the probable counterparts associated with the GRBs just within a few hours of occurrence. Indeed, the BeppoSax measurements allowed the detection of the fading X-ray emission, which follows the higher energy photon emission associated with the GRB in its highest state. Such an emission has been called *afterglow* (Costa et al., 1997) and extends at lower energy ranges, where the first Optical, IR, and Radio counterparts were detected since 1997 (e.g., reviews of Piran (1999a, 2000), Feroci (2001), Castro-Tirado (2002), and references therein). The first X-ray afterglow detected was that related to the GRB 970228 (Costa et al., 1997). This was one of the most important measurements performed in the space. A previously unknown X-ray source was seen to vary by a factor of 20 on a 3 days timescale. Figure 12 shows such an event.

The precise X-ray position (1′) triggered the research for the eventual optical afterglow (OA), which was actually detected by Pedichini et al. (1997) and Guarnieri et al. (1997) in the rising phase of the light curve. The optical maximum ($V \sim 21.3$ mag was reached $\sim$ 20 hours after the GRB maximum emission (Groot et al., 1997) and the power law

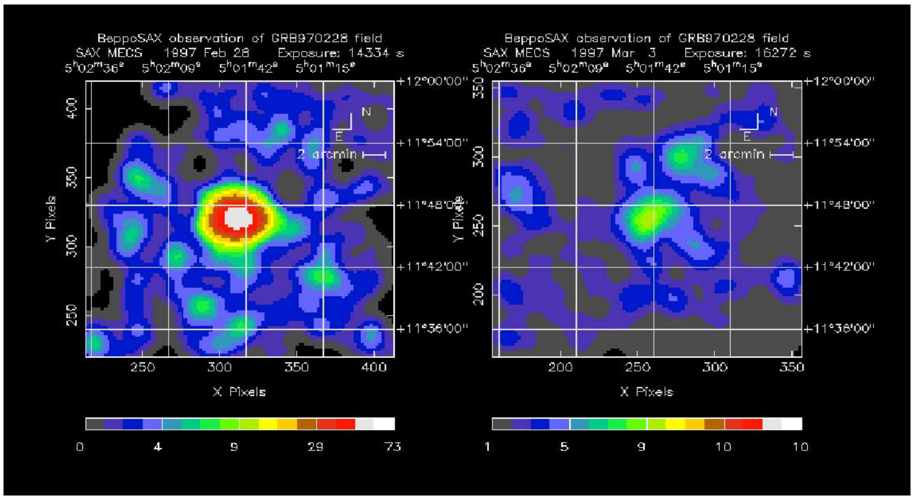

Fig. 12. X-ray afterglow of the GRB 970228, from BeppoSAX (Costa et al., 1997; courtesy of Enrico Costa and the BeppoSAX GRB Team).

decay was best fitted by $F \propto t^{-1.2}$ (Galama et al., 1997; Bartolini et al., 1998). An extended source was seen at the OA position by ground based and HST observations (van Paradijs et al., 1997; Sahu et al., 1997). Six months later HST detected in the position of the OA an object having $V = 28$ mag as well as the extended source with $V = 25.7$ mag (Fruchter et al., 1997). The extended source surrounding the point source was interpreted as a galaxy. Later, the redshift of such a galaxy was determined as $z = 0.695$ (Djorgovski et al., 1999). Reichart (1999) proposed a type Ib/c supernova lies 'behind' the GRB, overtaking the light curve two weeks after. This has been confirmed by Galama et al. (2000).

With the detection of the afterglow of the GRB 970228, the so called Afterglow Era for GRBs started. A confirmation that this Era was born arrived soon with the detection of the radio afterglow of the GRB 970508 (Frail et al., 1997), whose distance was derived by the optical spectrum as $z = 0.835$ (Metzger et al., 1997). So the 30 year old problem of fixing the distances to the GRB sources was apparently solved.

For the GRB 990510, following the BeppoSAX/WFC detection, Vreeswijk et al. (1999a,b) found the optical counterpart placed at $z = 1.619$. This is the first GRB for which polarized optical emission was detected ($1.7 \pm 0.2\%$) $\sim$ 18.5 hr after the maximum emission (Covino et al., 1999) and later on by Wijers et al. (1999). This confirms the synchrotron origin of the blast wave itself and represents the second case for jet-like outflow (Stanek et al., 1999), being the first that of the GRB 970228.

Thus GRB counterparts are multifrequency emitters, contrary supernovae, which emit most of their energy at the optical frequencies. The X-ray and optical afterglows of GRBs have been discussed in two excellent review by Frontera (2003) and Pian & Hjorth (2003), respectively.

Costa (1999) discussed on the X-ray afterglows of GRBs, detected with BeppoSAX. They pointed with the Narrow Field Instrument (NFI) at 12 directions of the 14 detected GRBs, at that time. In almost all cases they detected X-ray sources which, in the large majority they associate with the GRB, owing to their temporal behaviour. For a large fraction of these GRBs, transient sources in other wavelengths and host galaxies have been detected. They review the main spectral and temporal features of these afterglow sources, their energetics and

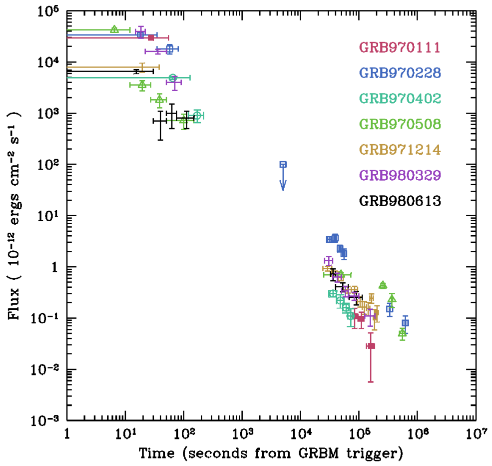

Fig. 13. The decay of the flux of the most luminous BeppoSAX GRB X-ray afterglows (Credit: Costa, et al., A&ASS, 138, 425, 1999, reproduced with permission © ESO).

the association with other features. Figure 13 shows the decay of most luminous afterglow sources. The lines on the left side of the plot indicate the average flux in the 2–10 keV band during the main burst itself.

The SWIFT observatory is strongly improving our knowledge about GRBs. The average redshift of the host galaxies for the long GRBs is $\bar{z} = 2.3$, which is a factor of ~ 2 greater than the average redshift for the GRBs detected in the pre–SWIFT era (Malesani, 2006). Moreover, this spacecraft has detected few dozens short bursts at cosmological distances at average redshift $\bar{z} = 0.5$. They are located mostly in elliptical galaxies outside of the star formation regions. Therefore, they must be connected to the old population and not to the young massive stars (as the long bursts are). The most likely explanation is that at least large part (majority?) of these events are due to mergers of compact objects (e.g. Ziółkowski, 2007).

Theoretical description of GRBs is still an open strongly controversial question. Fireball (FB) model (Meszaros & Rees, 1992; Piran, 1999b), cannon ball (CB) model (Dar & De Rújula, 2004), spinnin-precessing jet (SPJ) model (Fargion, 2003a,b) are the most popular, but each one against the others. Dar (2006) critically discussed the FB and CB models. He concluded that the CB model is incredibly more successful than the standard FB models of GRBs. Fargion & Grossi (2006) support the validity of SPJ model declaring that it is even more general than the CB one.

2.1.3. Data bases and/or literature observations

Up–to–date there are numerous data bases of different space– and ground–based experiments, and a huge amount of literature reporting data acquired with many instruments in energy bands spread over the whole electromagnetic spectrum for a big amount of cosmic sources belonging to the most various classes of objects. Therefore, if one likes to understand the whole behaviour of a cosmic source, it is convenient to look at data bases and literature for the benefit of science. Indeed, it is possible to find an interesting huge store of data, and sometimes these data can be also by chance simultaneous, or coordinated.

An interesting example is that of the TTauri star RU Lupi, for which multifrequency coordinated (no-simultaneous) observations allowed to solve the problem of the rotational period, which is wrongly reported in the literature as $\sim$ 3.7 days (Plagemann, 1969; Boesgaard, 1984). Giovannelli et al. (1991), analyzing a large set of data from RU Lupi did not find any significant periodicity at 3.7 days. Giovannelli (1994) during the preparation of a review paper about RU Lupi, found in the literature several Flare–Like–Events (FLEs) in optical. These events, together with those obtained simultaneously in UV, optical, and IR (Giovannelli et al., 1987), and in X–ray (Giovannelli et al., 1984) showed a periodicity of $P_{FLE} = 27.686 \pm 0.002$ days, probably associated with the rotational period of the star. Indeed, if we put such a period in the diagram $\log L_x$ vs $\log v_{rot}$ (Bouvier, 1990), RU Lupi fits perfectly the relationship to which pre–main–sequence–stars obey, contrary to the wrong position in the diagram in which RU Lupi lies in the case that a period of

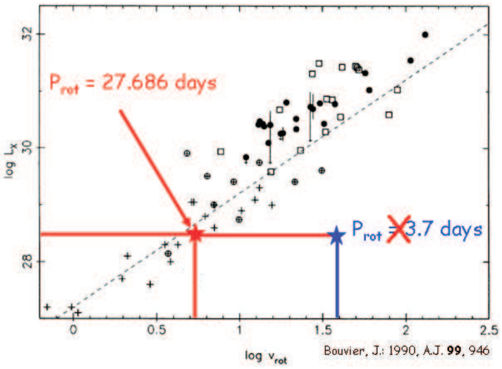

Fig. 14. X–ray luminosity versus rotational velocity of PMSSs (Bouvier, 1990). The position of RU Lupi is marked in red for rotational period of 27.686 days and in blue for 3.7 days (after Giovannelli, 1994).

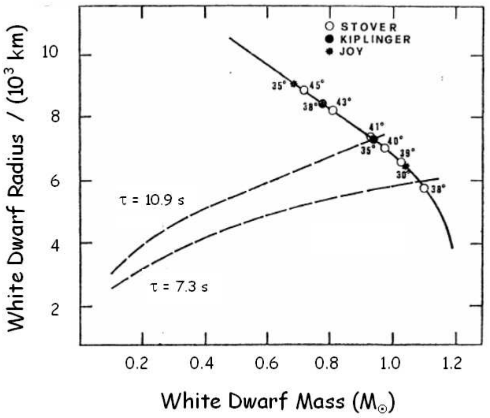

Fig. 15. Mass–Radius relationship for white dwarfs. Continuous line is from Hartle & Thorne theoretical calculations. Dashed lines refer to the maximum and minimum period of optical oscillations detected in SS Cygni. The open circles, black dots and asterisks refer to values coming from Stover et al. (1980), Kiplinger (1979), and Joy (1956), respectively, for different values of the orbital inclination angle (after Giovannelli et al., 1983).

3.7 days is taken as rotational one (see Figure 14).

2.1.4. Multifrequency observations (not necessarily simultaneous)

Multifrequency observations, although not simultaneous, can produce results useful to constrain some parameters of the studied systems. We will briefly discuss few examples.

2.1.4.1. Cataclysmic variables

SS Cygni is the most observed cataclysmic variable, since the end of the 19th century (Mattei et al., 1985), thanks to its high luminosity and to its position in the northern sky ($\alpha_{2000} = 21^h42^m42^s.804$; $\delta_{2000} = +43°35'09''.88$). In spite of this there are still controversial opinions about its nature – magnetic or not – and its orbital parameters, which were determined by Giovannelli et al. (1983) (FG83), by using different physical constraints, and later confirmed by Martinez–Pais et al. (1994) through radial velocities measurements of Balmer and other emission lines. How orbital parameters were determined: by using the doubling detected in the Balmer lines in emission, the projected circular velocity of matter in the outer edge of the accretion disk is $v_d \sin i = 192 \pm 10$ km s^{-1}. Assuming that the rotation of the disk is Keplerian, the radius of the disk is (Robinson, 1976):

$$R_d/a = (K/v_d \sin i)^2(1+q)/q^2$$

where a = separation of the centers of mass, R_d = radius of the disk, q = M_{WD}/M_R (white dwarf – late-type star mass ratio), K = the observed semiamplitude of the orbital radial velocity curve of the emission lines.

By using the observed semiamplitudes of the orbital radial velocity curves of the emission lines measured in optical by Stover et al. (1980) (S), Kiplinger (1979) (K), and Joy (1956) (J), the known upper and lower limits for the orbital inclination angle, FG83 constructed a grid of possible values for the separation of the two stars in the system (a), mass and radius of the secondary late–type star (M_R, R_R), the primary white dwarf star (M_{WD}, R_{WD}), and the dimension of the accretion disk around the white dwarf (R_d) in units of solar parameters. Then, considering the lower and upper values of the optical pulsations (7.3 s and 10.9

	i (deg)	50	45	44	43	42	41	40	39	38	35
$(a/10^{10})$ cm	S	12.0	13.0	13.2	13.5	13.7	14.0	14.3	14.6	14.9	16.0
	K	9.9	10.7	10.9	11.1	11.4	11.6	11.8	12.1	12.3	13.3
	J	11.8	12.7	13.0	13.2	13.5	13.7	14.0	14.3	14.6	15.7
$M_R/M_\odot$	S	0.33	0.42	0.45	0.47	0.50	0.53	0.56	0.60	0.64	0.79
	K	0.22	0.27	0.29	0.31	0.32	0.34	0.36	0.39	0.42	0.52
	J	0.44	0.57	0.60	0.63	0.67	0.71	0.75	0.80	0.86	1.06
$M_{wd}/M_\odot$	S	0.57	0.73	0.78	0.81	0.86	0.93	0.97	1.04	1.11	1.37
	K	0.29	0.37	0.39	0.42	0.43	0.46	0.49	0.52	0.56	0.69
	J	0.40	0.51	0.54	0.57	0.60	0.64	0.68	0.72	0.77	0.95
$R_R/R_\odot$	S	0.57	0.62	0.63	0.64	0.66	0.67	0.68	0.70	0.71	0.77
	K	0.50	0.54	0.56	0.57	0.58	0.59	0.60	0.62	0.63	0.67
	J	0.66	0.71	0.72	0.74	0.75	0.77	0.78	0.80	0.82	0.88
$R_d/R_\odot$	S	2.40	2.60	2.65	2.70	2.75	2.80	2.86	2.92	2.99	3.20
	K	2.58	2.78	2.84	2.89	2.96	3.02	3.07	3.14	3.21	3.43
	J	11.20	12.10	12.30	12.50	12.80	13.00	13.30	13.60	13.90	14.90

Fig. 16. Derived parameters for various orbital inclination angles. S, J, and K indicate the parameters derived from the observed semiamplitudes of the orbital radial velocity curves of the emission lines (after Giovannelli et al., 1983).

s), the Hartle & Thorne (1968) theoretical calculations (known at that time) of the mass–radius relationship for white dwarfs, the X–ray pulsation (9.7 s) detected by Patterson, Robinson & Kiplinger (1978), FG83 limited the possible values of the orbital parameters — under the hypothesis that the X-ray pulsation is due to the matter in Keplerian orbit around the white dwarf and then the mass of white dwarf would be $> 0.9\ M_\odot$ — to the following values: i = 40° (+1°, -2°), a = 14.3×10^{10} cm, $M_R = 0.56\ M_\odot$, $M_{WD} = 0.97\ M_\odot$, $R_R = 0.68\ R_\odot$, $R_d = 2.86 \times 10^{10}$ cm. The grid of values constructed by FG83 is shown in Figure 16, where the rows and column of the 'true' values of the orbital parameters are marked in red.

The upper limit of the white dwarf radius was determined by FG83 as $R_{in} < 3.6\times10^9$ cm. This value was later corroborated by Martinez–Pais et al. (1994) who found the radius of the white dwarf as $R_{WD} = 5 \times 10^8$ cm.

2.1.4.2. Background in the Universe

After the Big Bang the Universe started to expand with a fast cooling. The cosmic radiation observed now is probably a melting of different components which had their origin in different stages of the evolution as the results of different processes. This is the Diffuse Extragalactic Background Radiation (DEBRA), which, if observed in different energy ranges, allows the study of many astrophysical, cosmological, and particle physics phenomena.

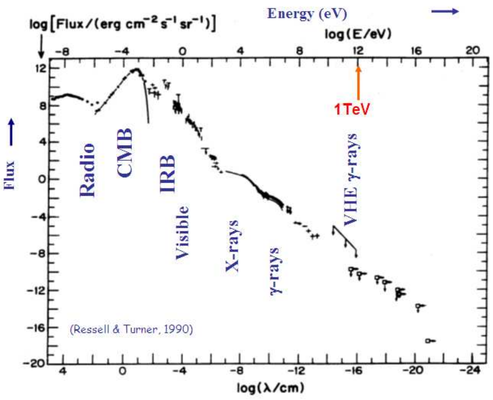

Fig. 17. The Grand Unified Photon Spectrum of the Diffuse Extragalactic Background Radiation (after Ressel & Turner, 1990).

It is possible to consider the DEBRA as a radiation produced by a cosmic source: the

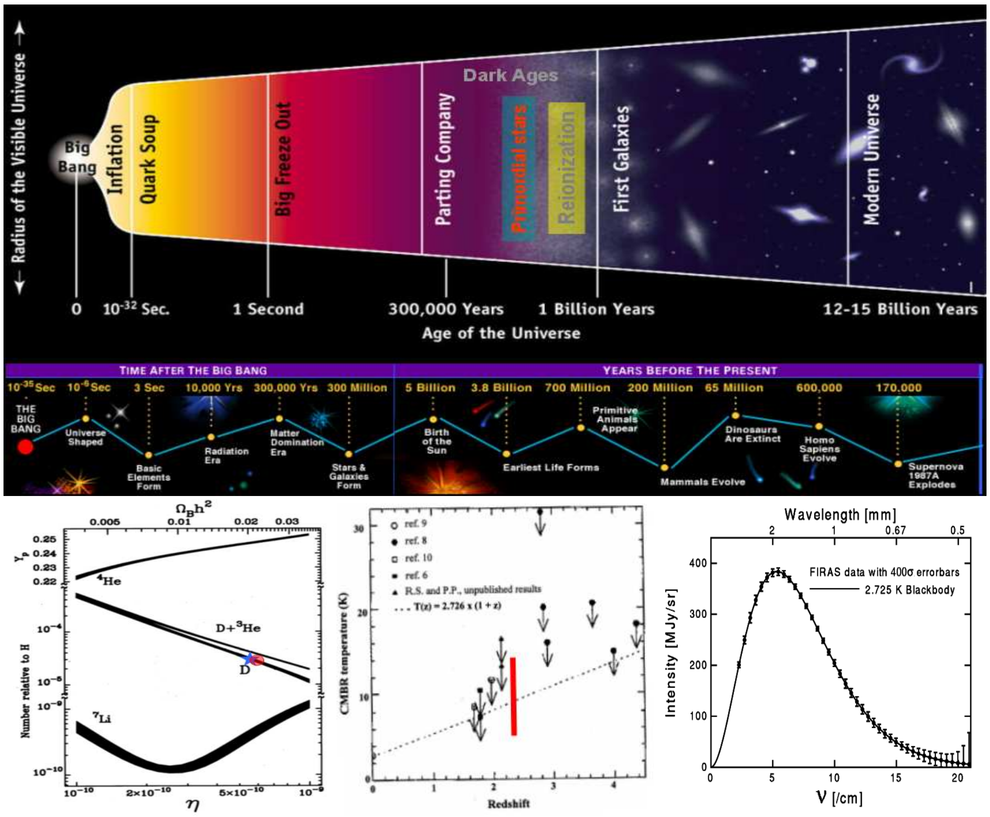

Fig. 18. Upper panel: Sketch of the evolution of the Universe with the main steps (adapted from Board of Trustees, University of Illinois, 1995, and Nino Panagia, 2006). Lower panel: Left - Light element abundances (after Burles, Nollett & Turner, 2001). Derived points from experiments are overlapped: ⋆ (Netterfield et al., 2002), ∘ (de Bernardis et al., 2000). Center - CMBR temperature versus redshift (after Srianand, Petitjean & Ledoux, 2000). Right - COBE–FIRAS 2.725 K black body spectrum (Mather etal., 1994).

whole Universe. Such a background radiation from radio to VHE γ-ray energy bands has been deeply discussed by Ressel & Turner (1990), Henry (1999, 2002), Miyaji, Hasinger & Schmidt (2000), and in the review paper by Giovannelli & Sabau-Graziati (2004). The analysis of the different components of DEBRA leads to the Grand Unified Photon Spectrum (GUPS), covering 29 orders of magnitude of the electromagnetic spectrum, from 10^{-9} to 10^{20} eV, as shown in Figure 17. The GUSP is continuously being updated, thanks to results coming from the many experiments in different energy regions. Henry (1999, 2002) thoroughly discussed the updated experimental situation of the cosmic background. DEBRA is the witness of the whole history of the Universe from the Big Bang to present time. Such history is sketched in Figure 18 (upper panel: Board of Trustees, University of Illinois, 1995, and Nino Panagia, 2006). In the lower panel there are the experimental measurements supporting the Big Bang theory. Indeed, in the left panel: the light element abundances (Burles, Nollett & Turner, 2001); in the lower center panel: the CMBR temperature at various redshifts as determined by Srianand, Petitjean & Ledoux (2000), and the references therein.

At $z = 2.1394$ there is an upper limit. At $z = 2.33771 \simeq 2.34$, the CMBR temperature is: $6.0 \text{ K} < T_{\text{CMBR}}(2.34) < 14.0 \text{ K}$ (vertical red bar). The dashed line is the prediction from the Hot Big Bang: $T_{\text{CMBR}} = T_{\text{CMBR}}(0) \times (1 + z)$. Such a prediction gives $T_{\text{CMBR}}(2.34) = 9.1$ K, which is consistent with the measurement. The point at $z = 0$ is the result of COBE ($T_{\text{CMBR}}(0) = 2.725 \pm 0.010$ K), which is well fitted by a black body spectrum, as shown in the lower right panel (Mather et al., 1994).

2.1.4.3. Multifrequency astroparticles

The Universe manifests not only through electromagnetic radiation but also through astroparticles, which are produced in different kinds of cosmic sources, and in different epochs of its history. By means of Earth-based experiments we are attempting to reproduce the most energetic events similar to those occurred after the Big Bang. Figure 19 shows schematically the temperature of the Universe versus time after the big Bang (Denegri, 2006). Different epochs with relative particles and ground–based experiments are superimposed.

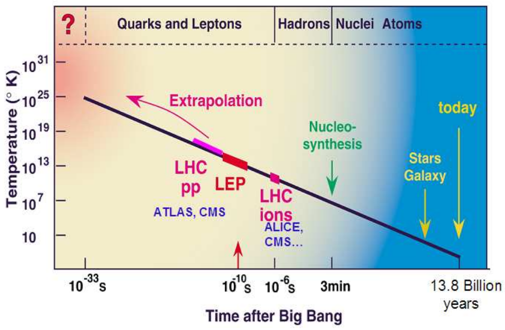

Fig. 19. Connecting the LHC and the Universe: towards the origin (courtesy of Denegri, 2006).

Important results can come from the study of galaxy clusters, the largest bound structures in the universe. They are the largest storage rooms for cosmic material (galaxies, dark matter (DM), hot thermal plasma, non-thermal and relativistic plasma, black holes (BHs), magnetic fields, cosmic rays (CRs)). In this sense they can be considered as the largest laboratories for Astroparticle Physics in the universe. In such laboratories one can efficiently study some of the most interesting aspects of the astroparticle physics of large scale structures (LSS): the nature of DM, the origin and distribution of CRs, the impact of magnetic fields on the evolution of LSS, the impact of BHs on LSS, the interplay between thermal and non-thermal phenomena in LSS. Two approaches can be used for studying these phenomena: i) a multi-frequency study of the various emission mechanism related to the previous phenomena; ii) a multi-purpose technique, i.e. the Sunyaev-Zeldovich (SZ) effect in its most general derivation (Colafrancesco, 2008).

The viable candidates proposed so far for a cosmologically relevant DM – neutralinos, sterile neutrinos, and more generally light DM particles – yield emission properties in DM halos that are markedly different and, therefore, allow a clear distinction of the relative DM nature.

Neutralinos which annihilate inside a DM halo produce quarks, leptons, vector bosons and Higgs bosons, depending on their mass and physical composition. Electrons are then produced from the decay of the final heavy fermions and bosons. The different composition of the $\chi\chi$ annihilation final state will in general affect the form of the electron spectrum (see for details Colafrancesco & Mele, 2001; Colafrancesco, 2006; Colafrancesco, Profumo & Ullio, 2006). The basic astrophysical mechanisms coming from the $\chi\chi$ annihilation are reported in Figure 20. It is possible to see that all the electromagnetic spectrum could be involved for detecting the products coming from the different astrophysical processes (Colafrancesco, 2007).

The hadronic products of their annihilation ($\chi\chi \rightarrow X + \pi^0 \rightarrow \gamma\gamma$) provide a prompt gamma-ray emission with a characteristic spectrum peaked around the π^0 threshold energy and dying off at the neutralino mass energy scale.
The leptonic products of neutralino annihilation (secondary electrons produced through various prompt generation mechanisms and by the decay of charged pions $\pi^\pm \rightarrow \mu^\pm \nu_\mu(\bar{\nu}_\mu)$, with $\mu^\pm \rightarrow e^\pm + \bar{\nu}_\mu(\nu_\mu) + \nu_e(\bar{\nu}_e)$ are instead sub-

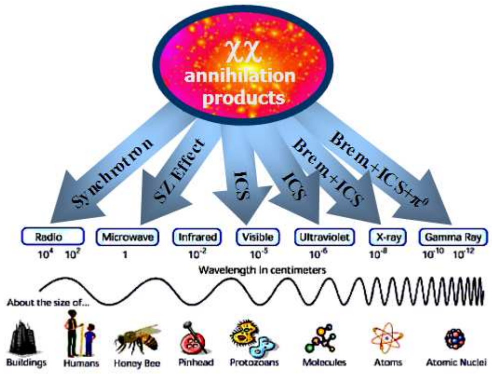

Fig. 20. The basic astrophysical mechanisms underlying the search for the nature of DM particles (χ) through the emission features occurring in large-scale structures (e.g., galaxy clusters and galaxies). These mechanisms are, among others: γ-ray emission from $\pi^0 \rightarrow \gamma + \gamma$, relativistic bremsstrahlung of secondary $e^{\pm}$ and ICS of CMB photons by secondary $e^{\pm}$; X-ray/UV emission due to non-thermal bremsstrahlung and ICS of background photons by secondary $e^{\pm}$; synchrotron emission by secondary $e^{\pm}$ diffusing in the intra-cluster magnetic field; SZ_{DM} (ICS of CMB photons by secondary $e^{\pm}$) effect (courtesy of Colafrancesco, 2007).

ject to spatial diffusion and energy losses. Both spatial diffusion and energy losses contribute to determine the evolution of the source spectrum into the equilibrium spectrum of these particles, *i.e.* the quantity which will be used to determine the multifrequency spectral energy distribution induced by $\chi\chi$ annihilation (Colafrancesco, 2008).

2.1.5. Multisites observations

Multisites observations are extremely useful in order either: i) to enhance the probability of success of ground-based observations either in the same energy region or not; or: ii) to follow a selected source continuously during long time, with telescopes at different geographical longitudes. In this case the night-day cycle is absent in all, while it is obviously present in each site.

We will briefly discuss both kinds of multisites observations.

2.1.5.1. MUSICOS (MUlti-SIte COntinuous Spectroscopy)

The spectroscopic sites involved in the MUSICOS 1998 campaign have been: INT (Isaac Newton Telescope, La Palma, Spain), OHP (Observatoire de Haute–Provence, France), XING (BAO: Beijing Astronomical Observatory, Xinglong, China), KP (Kitt Peak, USA), MTS/MSO (Mt. Stromlo, Australia), LNA (Labóratorio Nacional de Astrofísica, Itajubá, Brasil), ESO (La Silla, Chile), and SAAO (Cape Town, South Africa).

Garcia-Alvarez et al. (2003) performed simultaneous and continuous observations of the RS CVn system HR 1099. The spectroscopic observations were obtained during the MUSICOS 1998 campaign involving the former observatories and instruments. During this campaign, HR 1099 was observed almost continuously for more than 8 orbits of $2^{d}.8$. Two large optical flares were observed. A lower limit to the total flare energy of 1.3×10^{34} erg and 5.5×10^{34} erg for the first and second flare, respectively, comparable to other RS CVn flares. Contemporary photometric observations were carried out with the robotic telescopes APT-80 of Catania and Phoenix-25 of Fairborn Observatories. Maps of the distribution of the spotted regions on the photosphere of the binary components were derived. Figure 21 shows the maps of the distribution along stellar longitude of the spot filling factors at five rotation phases. Spots located at latitude below $\simeq -33°$ cannot contribute to the flux because the inclination of the star's rotation axis is 33°.

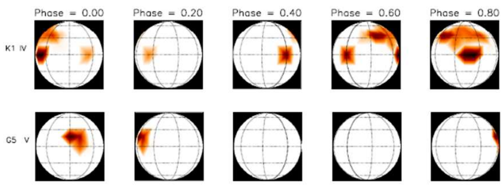

Fig. 21. Maps of the distribution along stellar longitude of the spot filling factors at five rotation phases of HR 1099 (Credit: Garcia-Alvarez et al., A&A, 397, 285, 2003, reproduced with permission © ESO).

Rotational modulation was observed in Hα and HeI D_3 in anti-correlation with the photometric light curves. Both flares occurred at the same binary phase (0.85), suggesting that these events took place in the same active region. Simultaneous X-ray observations were performed with ASM on board RXTE. A clear variability on short and long time-scales was observed. A number of flares and flare-like events were detected, some of which correlated well with the optical observations. Most of the X-ray events observed, took place either at $\phi \sim 0.31$ or at $\phi \sim 0.91$ (see Figure 22). It is possible to compare these results with Doppler Imaging based on the photospheric lines, to study the connection between spots, chromospheric emission and flares.

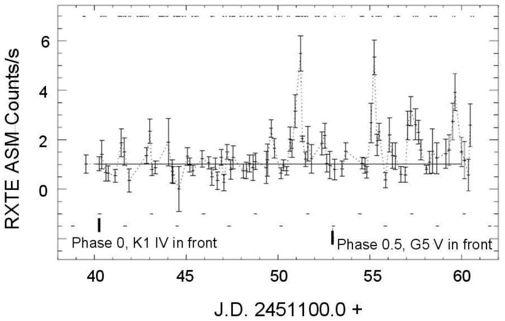

Fig. 22. X-ray light curve observations of HR 1099, from the ASM instrument on RXTE satellite, obtained at the same time as the MUSICOS 98 campaign. The band S (1.5-12 keV) as a function of Julian date is shown. The spectroscopic optical observations during MUSICOS 98 campaign are shown on top of the X-ray data (Credit: Garcia-Alvarez et al., A&A, 397, 285, 2003, reproduced with permission © ESO).

2.1.5.2. WET (Whole Earth Telescope)

In 1968 A. Landolt accidentally discovered the first pulsating hydrogen–rich white dwarf star HL Tau 76 (Landolt, 1968). Soon after, investigations started in order to find luminosity variations in white dwarfs, and they were found rendering theoreticians despaired. With the advent of a two–channel photometer it appeared clear that most of the variations previously detected were due to Earth's atmosphere. Robinson & McGraw (1976) with the new photometer found 8 real pulsators, which seemed to be hydrogen–rich white dwarfs (DAVs) and 35 non–pulsators of the same kind. For a short review see Solheim (2003). The variations in optical are very small — order of milli–magnitudes — therefore in order to avoid misunderstanding in the interpretation of data due to undersampled data, it appeared necessary to perform observations as long as possible. This is the main reason for originating the WET (Whole Earth Telescope) idea. This consists in generating a world–wide network of cooperating astronomical observatories to obtain uninterrupted time–series measurements of variable stars. The experimental objective was to resolve the multi–periodic oscillations into their individual components. Then, the asteroseismology born. Asteroseismology of stellar remnants is traditionally the study of the interior structure of pulsating white dwarfs and subdwarfs as revealed by global stellar oscillations. The oscillations allow a view beneath the photosphere, and contain information about basic physical parameters, such as mass, rotation rate, internal transition profiles, and compositional structure. This information provides important constraints on fields ranging from stellar formation and evolution, chemical evolution in our galaxy, the age of the galactic disk, the physics of Type Ia supernovae, and neutrino physics.

The WET, is an existing telescope, which comes into life one or two times every year. It consisted of astronomers who traveled to telescopes at the selected longitudes around the Earth to observe the same stars with functionally equivalent instruments. The observations were coordinated from the Texas headquarters and the stars observed were pulsating white dwarfs or other objects for which a long, nearly continuous, light curve is needed (Meištas & Solheim (eds.), 1993). Now, instead of students traveling from Texas, observers come from all over the world.

It is important to pay homage to Roy Edward Nather (Ed) who was the founder of the WET (Solheim, 1993).

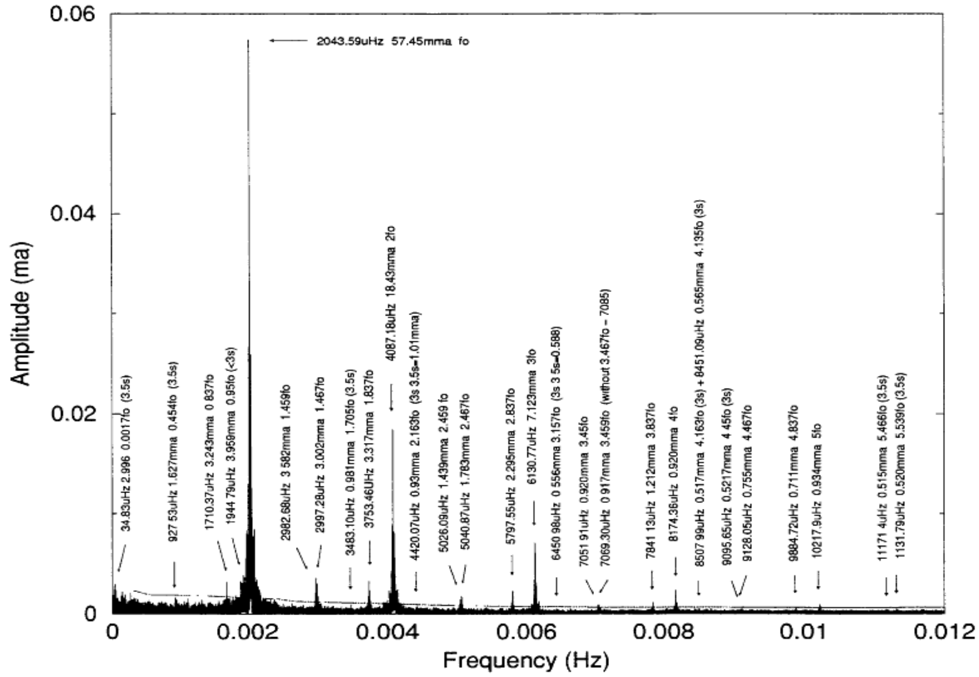

Fig. 23. The Fourier transform of the PG 1351+489 WET data with weights (Alves et al., 2003) (courtesy of Virginia Alves).

Since the evolution of white dwarf stars is characterized by cooling, asteroseismological studies of He atmosphere white dwarf pulsators (DBVs) give us opportunities to study white dwarf structure at a different evolutionary stage than the H atmosphere white dwarf pulsators (DAVs). The hottest DBVs are thought to have neutrino luminosities exceeding their photon luminosities (Winget et al. 2004), a quantity measurable through asteroseismology. Therefore, they can also be used to study neutrino physics in the stellar interior (Nitta et al., 2009a). Nitta et al. (2009b) have discovered nine new DBVs, doubling the number of previously known DBVs.

The DBVs are commonly thought to be the descendants of the hotter PG 1159 stars, which initially have uniform He/C/O atmospheres. In this evolutionary scenario, diffusion builds a pure He surface layer which gradually thickens as the star cools. In the temperature range of the pulsating DB white dwarfs ($T_{eff} \sim 25,000$ K) this transformation is still taking place, allowing asteroseismic tests of the theory (Metcalfe et al., 2005).

Figure 23 shows, as example, the Fourier transform of the PG 1351+489 WET data (1995 XCov12 campaign) corrected with weights (Alves et al., 2003). PG 1351+489 was discovered by Winget, Nather & Hill (1987) and they proposed it to be the most simple and stable light curve pulsating DBV white dwarf. The dominant peak at $\nu_0 = 489.5$ s and its first and second harmonics were detected. Also a small peak at 333 s, corresponding to 1.47 ν_0 as well as 2.47 ν_0 and 3.47 ν_0, at smaller amplitudes. These small amplitude peaks varied in amplitude with time, although their frequencies were the same whenever they could be detected. The goal of the 1995 campaign was that of resolving the detected frequency bands into individual frequencies and revealing other regions of lower power by means of better signal–to–noise ratio. These developments allowed seismic analysis, together with other data. Indeed, Alves et al. (2005) fitted the 1996 HST FOS and the 1985 IUE ultraviolet spectra of PG1351+489 with theoretical models for the flux curves as functions of wavelength, to obtain the best values for T_{eff} and log g. They found $T_{eff} = 24,018 \pm 280$ K and log g $= 7.70 \pm 0.06$ for the HST data and $T_{eff} = 22,470 \pm 262$ K and log g $= 7.78 \pm 0.06$ for the IUE data. The fitting also allowed the determination of the distance of the star: for a radius of R = 9000 km, consistent with this mass and temperature, they found a distance of 181 ± 7 pc for HST data and 169 ± 31 pc for IUE data.

The He atmosphere sub–dwarfs (SdBs) are believed to be the field counterparts of the Extreme Horizontal Branch stars in globular clusters and have a canonical mass of 0.5 $M_\odot$, even though there is still some debate concerning their mass distribution and their prior evolution, especially including binary formation. Their helium core, feeding the 3α–cycle nuclear fusion, is surrounded by a thin hydrogen envelope ($M \leq 0.02\ M_\odot$). In 1997, pulsations in sdBs were predicted (Charpinet et al. 1996), and detected observationally (e.g. Kilkenny et al. 1997; Piccioni et al., 2000).

The presence of stellar oscillations in sdBs opened up the possibility of employing asteroseismological techniques for this group of evolved objects (e.g. Charpinet et al. 2005a,b; Oreiro et al. 2005).

Dolez et al. (2006) analysed the WET observations of HL Tau 76, the first discovered pulsating DA white dwarf. The star was observed during two WET campaigns. With a total duration of 18 days, the frequency resolution achieved is 0.68 μHz. With such a frequency resolution, they found a total of 43 independent frequencies. This makes HL Tau 76 the richest ZZ Ceti star in terms of number of observed pulsation modes. They use those pulsation frequencies to determine as much as possible of the internal structure of HL Tau 76. The pulsations in HL Tau 76 cover a wide range of periods between 380 s and 1390 s. Their results constitute a starting point for a detailed comparison of the observed periods with the periods calculated for models as representative as possible of HL Tau 76.

BPM 37093 is the only hydrogen-atmosphere white dwarf currently known which has sufficient mass ($\sim 1.1 M_\odot$) to theoretically crystallize while still inside the ZZ Ceti instability strip (Teff $\sim 12,000$ K). As a consequence, this star represents our first opportunity to test crystallization theory directly. If the core is substantially crystallized, then the inner boundary for each pulsation mode will be located at the top of the solid core rather than at the center of the star, affecting mainly the average period spacing. Kanaan et al. (2005) reported WET observations of BPM 37093 obtained in 1998 and 1999. Based on a simple analysis of the average period spacing they conclude that a large fraction of the total stellar mass is likely to be crystallized.

2.2. Theoretical multifrequency astrophysics

Theoretical multifrequency astrophysics can be developed as follows: a) Wide-range Physical Processes; b) Narrow-range Physical Processes.

2.2.1. Wide-range physical processes

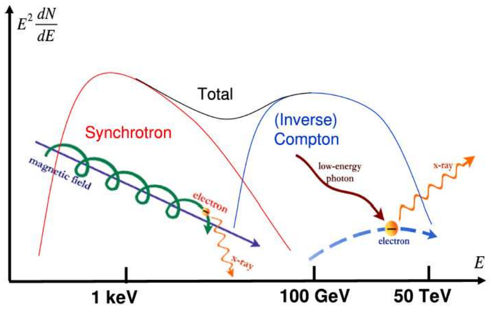

Fig. 24. Differential energy spectrum of photons in the self-synchrotron Compton (SSC) model (De Angelis, Mansutti & Persic, 2008) (reproduced with kind permission of Società Italiana di Fisica).

Wide-range physical processes are those processes which manifest their effects in a

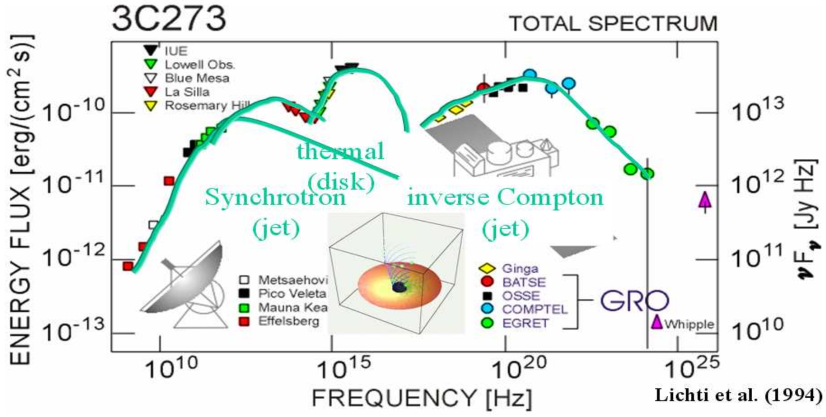

Fig. 25. Total experimental energy spectrum of 3C 273 best fitted with different components of the theoretical spectra. The many multifrequency data are coming from different experiments listed in the figure (after Lichti et al., 1994, 1995) (courtesy of Giselher Lichti).

wide range of the electromagnetic spectrum. Then, the theoretical spectra obtained can be used to fit multifrequency experimental data. Only if the fits to experimental data, spread in a wide energy range, are good, theoretical models can be accepted. This statement seems obvious, but sometimes, unfortunately, it is not so!

The source of high-energy photons from astrophysical objects is mainly gravitational energy released by collapses towards a central massive object. In the presence of angular momentum, the dynamics of such a collapse can manifest itself in an accretion disk, with the presence of jets of plasma out owing the accretion plane. In addition, one could have characteristic photon signals also from annihilation/decay of heavy particles. At the origin of the production of gamma-rays there is mostly the photon radiation of charged particles, in general electrons. Such a radiation might happen due to bremsstrahlung and synchrotron radiation. For ultra-relativistic electrons (typically encountered in astrophysical situations), the emission spectrum is powerlaw. High-energy synchrotron radiation can only originate in regions of very strong magnetic field, e.g. close to a neutron star surface (where $B \gtrsim 10^{12}$ G). Alternatively, primary photons can originate from nuclear transition, or decay of π° in a hadronic environment.

Photons can be produced also by gravitational collapses and by self-annihilation of dark matter. The basic interpretation for the production of high-energy photons from gravitational collapses is the so-called self-synchrotron Compton (SSC) mechanism. Synchrotron emission from ultra-relativistic electrons accelerated in a magnetic field generates photons with an energy spectrum peaked in the infrared/X-ray range. Such photons in turn interact via Compton scattering with their own parent electron population: since electrons are ultrarelativistic (with a Lorentz factor $\gamma_e \sim 10^{4-5}$), the energy of the upscattered photon gets boosted by a factor $\lesssim \gamma_e^2$. The upscattering of low-energy photons by collisions with high-energy electrons is the inverse Compton (IC) scattering. This mechanism is very effective for increasing the photon energy (for this reason it is called *inverse*, and is important in regions of high soft-photon energy density and energetic-electron number density. The Compton component can peak at GeV–TeV energies; the two characteristic synchrotron and Compton peaks are clearly visible on top of a general E_γ^{-2} dependence. Figure 24 shows the resulting energy spectrum (De Angelis, Mansutti & Persic, 2008). This behavior has been verified with high accuracy on the Crab Nebula, a steady VHE gamma emitter in the Milky Way which is often used to calibrate VHE gamma instruments.

Very impressive is the total spectrum of 3C 273 where the different components of the theoretical total spectrum fit successfully the numerous multifrequency data coming from different experiments, listed in the Figure 25 (Lichti et al., 1994, 1995).

2.2.2. Narrow-range physical processes

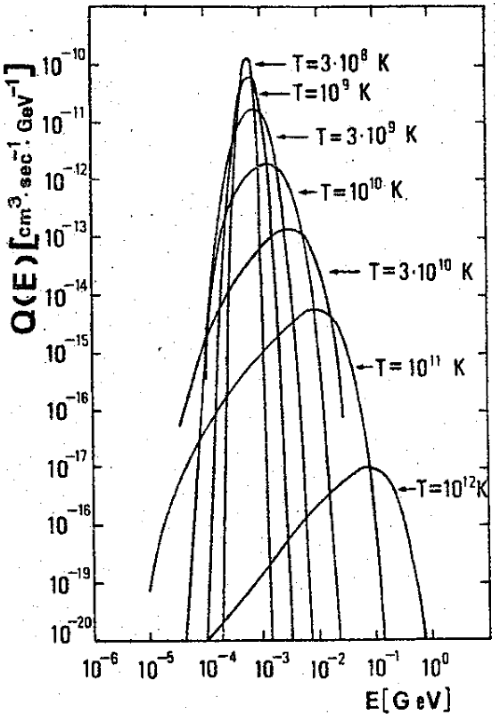

Fig. 26. The photon energy production spectra from e^+e^- annihilation process for selected temperatures and unit concentration of positrons and electrons in the plasma (Karakuła & Tkaczyk, 1985) (Courtesy of Edizioni Scientifiche Siderea, Roma).

Narrow-range physical processes are those processes which manifest their effects in a narrow range of the electromagnetic spectrum. These processes can explain some or all experimental behaviour of cosmic sources.

One example of a such physical process is the e^+e^- annihilation, which occurs in many classes of cosmic sources. The e^+e^- annihilation radiation at 0.511 MeV from the direction of the Galactic Center — first seen by Johnson, Harnden & Haymes (1972) with a low–resolution NaI detectors, and later by Leventhal, MacCallum & Stang (1978) with high–resolution Ge detectors in balloon–borne experiments — triggered the theoretical work of Karakuła & Tkaczyk (1985). Figure 26 shows the photon energy production spectra from e^+e^- annihilation process in a hot plasma for selected temperatures and unit concentration of positrons and electrons in the plasma, under the hypothesis that both electrons and positrons have Maxwellian momentum distributions at the same temperature and their angular distributions are isotropic (Karakuła & Tkaczyk, 1985). The shape of the calculated annihilation spectra depends on the temperature plasma. It is possible to note that the annihilation spectra have characteristic thermal cutoff at high energy sides. The peak energy of the annihilation spectrum as function of the plasma temperature is shown in Figure 27. The peak energy of annihilation line indicates a weak dependence on plasma temperature up to 3×10^9 K, but is is almost linear for greater temperatures.

The full width at half–maximum (FWHM) of annihilation spectra as function of plasma temperature is shown in Figure 28. The FWHM is $\sim$ 200 keV at T = 10^8 K and increases with the temperature

Another example can come from the research on dark matter. Indeed, the main field of research for dark matter in the γ-ray energy range is related to the detection of photons emitted by the self-annihilation of WIMPs. In particular, in supersymmetric models the lightest supersymmetric neutral particle, the neutralino, is predicted to be a Majorana particle, and is thus a natural candidate for such a WIMP. The self-annihilation of a heavy WIMP χ can generate photons (see Figure 29) in three main ways: i) directly via annihilation into a photon pair ($\chi\chi \rightarrow \gamma\gamma$) or into a photon –

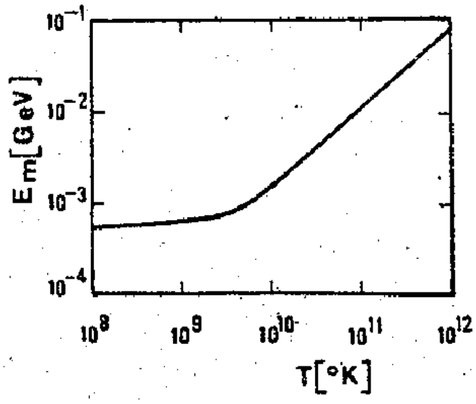

Fig. 27. The peak energy of e^+e^- annihilation spectrum (E_m) versus plasma temperature (Karakuła & Tkaczyk, 1985) (Courtesy of Edizioni Scientifiche Siderea, Roma).

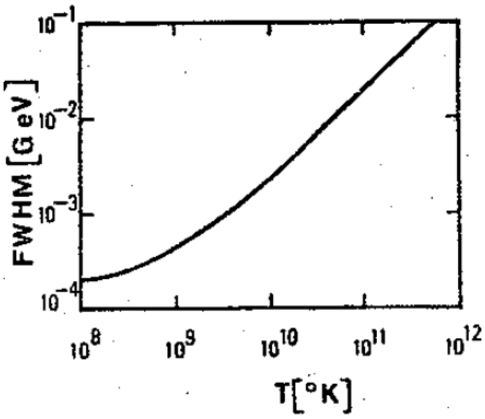

Fig. 28. FWHM of e^+e^- annihilation spectrum versus plasma temperature (Karakuła & Tkaczyk, 1985) (Courtesy of Edizioni Scientifiche Siderea, Roma).

Z-boson pair ($\chi\chi \rightarrow \gamma Z$). These processes give a clear signature at high energies, being the energy monochromatic, but the process is suppressed at one loop, so the flux is expected to be very faint; ii) via annihilation into a quark pair which produces jets emitting in turn a large number of γ photons (qq $\rightarrow$ jets $\rightarrow$ many photons); this process produces a continuum of γ-rays with energies below the WIMP mass; the flux can be large but the signature might be difficult to detect; iii) via internal bremsstrahlung (Bringmann, Bergström & J. Edsjö, 2007). Also in this case one has an excess of low energy γ-rays with respect to a background which is not so well known.

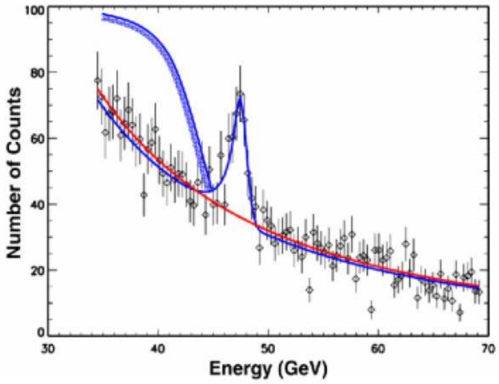

Fig. 29. Simulated signals of the WIMPs self-annihilation: a narrow peak or a continuum below the mass of the WIMP (De Angelis, Mansutti & Persic, 2008, after GLAST Science Brochure, 2001) (reproduced with kind permission of Società Italiana di Fisica).

3. Few remarkable notes

The most astonishing experimental events in the past decades have been the discovery of a well populated high energy sky, with 125 X-ray sources, detected by the UHURU satellite (Forman et al., 1978), and later with $\sim$ 1000 sources detected by the HEAO A-1 satellite (Wood et al., 1984). Similar trend was obtained looking at the γ-ray sky, starting with the COS B (25 sources) (Swanenburg et al., 1981) to EGRET-CGRO (271 sources) (Hartman et al., 1999).

FERMI observatory is revealing a very rich sky in the sub-TeV range (10 MeV – 300 GeV). In the first three months of observations FERMI has detected more than 200 sources (Abdo et al., 2009) – almost the same number of those reported in the whole EGRET catalog – rendering true the trend reported in the Kifune plot (Figure 30) for the number of sources potentially detectable by the observatory. The detection of VHE sources has been even more amazing, and up-to-date more than 75 sources, detected by different VHE experiments, are populating the sky. This is an important discovery, since such results push the high energy astrophysics toward the particle physics: both fields are the bulk of the newborn field of *Astroparticle Physics*.

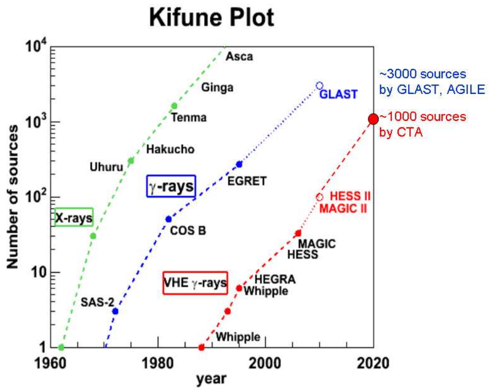

Fig. 30. Source numbers versus time in the X-ray, γ-ray and VHE γ-ray domains. Extrapolation of these numbers up to the year 2020 is reported too (courtesy of Bartko, 2007, adapted from a plot of Tadashi Kifune).

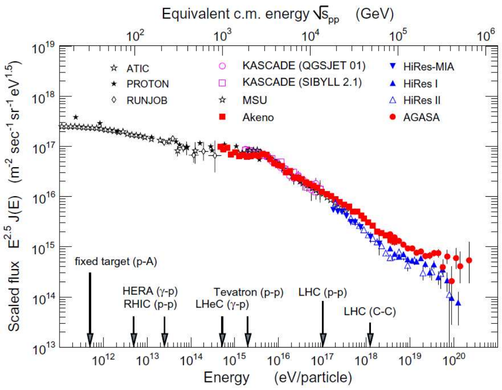

Fig. 31. Cosmic-ray total energy spectrum. Present and future accelerators are indicated with arrows (De Roeck, 2008) (Credit: Albert De Roeck & Ralf Engel (Karlsruhe)).

Figure 30 shows the increasing number of high energy cosmic sources detected by different HE space experiments versus time. It is interesting to note that the number of γ-ray and VHE γ-ray sources follow the trend of that of X-ray sources, with obvious scale factors due to the smaller number of photons for growing energies. The extrapolation up to the year 2020 is also reported together with the future space experiments (Bartko, 2007). Only fourteen years ago the VHE sky was practically empty with the three exceptions of the Crab Nebula, Mrk421, and Mrk501.

Figure 31 shows the cosmic ray total spectrum in which results of different experiments are reported with different colors. The arrows on the bottom line show the equivalent energies of the various accelerators experiments, either operational or where the construction is near completion (De Roeck, 2008).

Also for the cosmic rays, the energy ranges of the passive experiments are increasing toward higher and higher energies, up to the probable upper limits of order 10^{21} eV, well beyond the limits reachable with the active experiments, like LHC accelerator. The total spectrum of cosmic rays spans twelve orders of magnitudes in energy ($1 - 10^{12}$ GeV) and ten in flux ($\sim 10^{-6} - 10^{4}$ GeV m^{-2} sr^{-1} s^{-1}). This obliges an use of different technique of detection in function of the energy regions to be explored. Up to $\sim 10^2$ GeV the instruments used are spectrometers, having a good energy resolution. Up to $\sim 10^4$ GeV the instruments used are calorimeters, having lower resolution with respect to the spectrometers, and for energies $\geq 10^4$ GeV the air shower technique is used.

4. Prospects

4.1. The high energy sky

The high energy sky which was simply empty before the sixties is now populated by thousands UV and X-ray sources, as well as by hundreds HE γ-ray sources and by tens VHE γ-ray sources. At present FERMI observatory, in the first three months of observations, detected more than 200 sources, which are $\sim 75\%$ of the total number of sources in the EGRET catalog. So that, the numbers of γ-ray sources is raising like in the past X-ray sources did because of increasing sensitivities and sizes of VHE experiments (see Figure 4).

Also the experiments for measuring spectra and composition of cosmic rays at high energies rapidly developed, and results are deeply discussed by Stanev (2007a) and by different authors at the Aspen 2005 Workshop about *"Physics at the end of galactic cosmic ray spectrum"* (J. Phys.: Conf. Ser. 47, 1–270 (2006)), and summarized by Sokolsky (2006). Particularly important is the region of transition between galactic and extragalactic cosmic rays for which AUGER observatory is potentially able to provide high experimental statistics in their detection. A discussion can be found in Stanev (2007b). Recently, in a review paper, Blümer, Engel & Hörandel (2009) discussed the cosmic rays from the knee to the highest energies.

4.2. Gamma-ray astronomy as probe for cosmic-rays

A particular attention is necessary at the highest energies where the cosmic ray spectrum extends to $\geq 10^{20}$ eV (see Figure 31). Yet the origins of such spectacularly high energy particles remains obscure. Particle energies of this magnitude imply that near their acceleration sites a range of elementary particle physics phenomena is present which is beyond the ability of present day particle accelerators to explore. VHE γ-ray astronomy may catch a glimpse of such phenomena. As discussed by Stanev (2007c), the features of high energy cosmic rays detected with air shower observations, as well as the discussion about the sources and astrophysical acceleration, pointed at the same problem, which seems to worry many of us - where is the end of the galactic cosmic ray spectrum?

Important results at the highest energies are coming from Auger experiment: the spectral index γ of the particle flux $J \propto E^{-\gamma}$ is ~ 2.69 between 4×10^{18} eV and 4×10^{19} eV, and steepening to ~ 4.2 at higher energies (Abraham et al., 2008).

It is interesting in Figure 32 to look at the sensitivities of some present and future HE gamma detectors, measured as the minimum intensity source detectable at 5σ. The performance for EAS and satellite detector is based on one year of data taking; for Cherenkov telescopes it is based on 50 hours of data. The sensitivity curve for VERITAS is between MAGIC and MAGIC-2 (De Angelis, Mansutti & Persic, 2008). With the future CTA, the sensitivity is well below 0.01 Crab in the TeV range; this will substantially carry out our knowledge about the highest energy Universe.

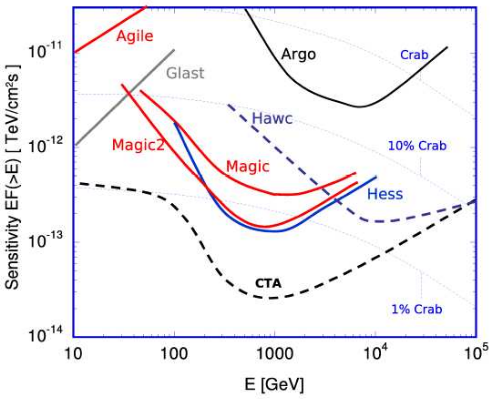

Fig. 32. The sensitivities of some present and future HE gamma detectors (De Angelis, Mansutti & Persic, 2008) (reproduced with kind permission of Società Italiana di Fisica).

4.3. Present and future experiments

We do not want to discuss ground–based cosmic–ray experiments. We invite the reader to look specialized papers, part of them discussed during the Vulcano Workshop 2006 (Giovannelli & Mannocchi, 2007) and others discussed in the session 'Direction for Next Generation Experiments' of the Vulcano Workshop 2008 (Giovannelli & Mannocchi, 2009). Another source of precious information about cosmic ray ground– and space–based experiments is coming from the Aspen 2005 Workshop (J. Phys.: Conf. Ser. 47, 1–270 (2006)).

Since most of the energy ranges are forbidden by ground–based observations, space–based experiments must be developed, follow-

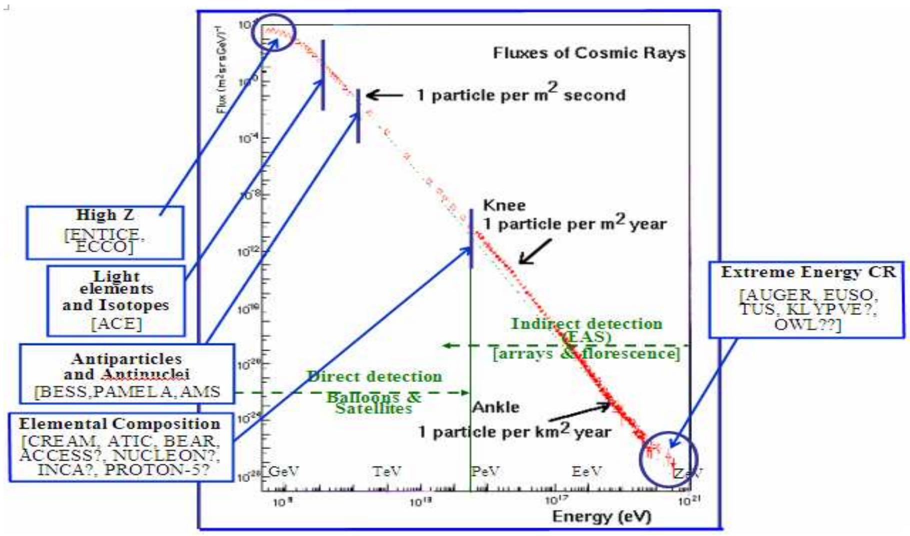

Fig. 33. Cosmic ray spectrum. The names of the experiments are superimposed. At energies below $\approx 10^{14}$ eV, cosmic rays, which are mainly protons, are detected by space experiments. At energies above $\approx 10^{14}$ eV measurements come from arrays of ground based detectors (Spillantini, 2007) (reproduced with kind permission of Società Italiana di Fisica).

ing the general trend in increasing their sensitivities, compatibly with reasonable costs. But the spectral resolution in most of the energy bands is very close to the theoretical one. So, only by increasing the dimensions of the detectors it will be possible to reach lower thresholds in intensities. An exception is the spatial resolution, that can be improved a lot by interferometric techniques.

Only genial ideas for new detectors could provide a significant step in increasing their performances.

4.3.1. Cosmic ray experiments in space

Several cosmic ray experiments in space have been planned in the last few years. Robert E. Streitmatter in his talk at the Aspen 2005 Workshop discussed such experiments. Giovannelli (2007) briefly described their main characteristics. Spillantini (2007) also discussed a wider sample of experiments (including some ground–based), being their names superimposed to the cosmic ray spectrum in correspondence of the energy where they will operate, as shown in Figure 33.

Few words about the problem of the UHECR astronomy at energies $\geq 10^{20}$ eV. Has the spectrum an end? There is a clear evidence of suppression of flux $> 4 \times 10^{19}$ eV, which is roughly in agreement with HiRes at highest energies. A key requirement is the identification of individual sources and measurement of their energy spectrum. However, we can expect some – but few ($\sim$ 1 with Auger) – events above 10^{20} eV, and only a few per millenium per km^2 above 10^{20} eV. Although it is impossible to predict what Auger will find in the next few years, it seems certain that it will be necessary to monitor massive volumes of atmosphere to study charged cosmic rays and neutrinos with energies above 10^{20} eV. Observations from a space platform are likely to be essential, particularly for the study of very high energy neutrinos.Then, in order to have chances to measure the characteristics of cosmic rays at such high energies it is necessary to be able to rich high exposure times, as high as $A_{exp} \geq 10^6$ Linsley (1 L = 1 km^2 sr yr), like with the future JEM-EUSO and Super-EUSO projects (Santangelo, 2008).

4.3.2. Photon experiments in space

In the study of cosmic sources, experiments with increasing resolutions (e.g. the X- and γ-ray missions ROSAT, ASCA, RXTE, BeppoSAX, CHANDRA, XMM, INTEGRAL, SUZAKU, AGILE, FERMI, and the next generation missions) are crucial for a better comprehension of the physics governing their behavior:

i) Resolution in Energy: better resolution allows the detailed studies of astrophysical plasmas and line profiles;

ii) Resolution in Position: increasing this resolution it is possible to distinguish close sources in a crowded field (i.e. Galactic Center X-ray sources). Future X-ray experiments could discern protoclusters and protogalaxies and finally, with interferometric techniques, it will be probably possible to look at accretion disks and stellar surfaces;

iii) Resolution in Sensitivity: increasing this resolution it is possible: a) to detect weaker sources (i.e. ROSAT detected more than 100,000 soft X-ray sources, most of them before ROSAT confused in the background radiation); b) to detect either flux variations at lower levels in a fixed Δt, or flux variations at higher levels but in shorter time scales.

The main high energy experiments (space– and ground–based), with their ranges of detection and their sensitivities from the beginning of 1990s to next decade (Morselli, 2007) are reported in Figures 5 and 6 of the review by Giovannelli (2007), respectively.

5. Conclusions

It is becoming increasingly clear that the energy régime covered by VHE γ-ray astronomy will be able to address a number of significant scientific questions, which include: i) What parameters determine the cut-off energy for pulsed γ-rays from pulsars? ii) What is the role of shell-type supernovae in the production of cosmic rays? iii) At what energies do AGN blazar spectra cut-off? iv) Are gamma blazar spectral cut-offs intrinsic to the source or due to intergalactic absorption? v) Is the dominant particle species in AGN jets leptonic or hadronic? vi) Can intergalactic absorption of the VHE emission of AGN's be a tool to calibrate the epoch of galaxy formation, the Hubble parameter, and the distance to γ-ray bursts? vii) Are there sources of γ-rays which are 'loud' at VHEs, but 'quiet' at other wavelengths?

It appears evident the importance of Multifrequency Astrophysics and Multienergy Particle Physics. There are many problems in performing simultaneous Multifrequency, Multienergy, Multisite, Multiinstrument, Multiplatform measurements due to: i) objective technological difficulties; ii) sharing common scientific objectives; iii) problems of scheduling and budgets; iv) politic management of science.

In spite of the many ground– and space–based experiments providing an impressive quantity of excellent data in different energy regions, many open problems still exist. We believe that only drastically changing the philosophy of the experiments, it will be possible to solve faster most of the present open problems. For instance, in the case of space–based experiments, small satellites — dedicated to specific missions and problems, and having the possibility of scheduling very long time observations — must be supported because of their relative faster preparation, easier management and lower costs with respect to medium and large satellites.

We strongly believe that in the next decades passive–physics experiments space– and ground–based will be the most suitable probes in sounding the physics of the Universe. Probably the active physics experiments have already reached the maximum dimensions compatible with a reasonable cost/benefit ratio, with the obvious exception of the neutrino–astronomy experiments.

6. DISCUSSION

JAMES H. BEALL: Can you comment on the originating region where the line emission is produced? Is it from the disk?

FRANCO GIOVANNELLI: You clearly refers to HeI optical emission lines detected in the Flavia' star, optical counterpart of the X-ray pulsar A0535+26. We suggest (Giovannelli et al., 2007, A&A, 475, 651) that HeI lines can be produced in a temporary accretion disk around the neutron star. Indeed, the HeI emission lines clearly show doubling, which is good evidence for the presence of a disk. We have critically discussed the possibility that this disk is a temporary accretion disk around the neutron star, a view that contrasts to the usual interpretation, which considers that this sort of doubling in the HeI emission lines is due to a disk formed by gas expelled from the Be star. The presence of such a temporary accretion disc around the neutron star was predicted by Giovannelli & Ziółkowski (1990, AcA, 40, 95), and later detected by Finger, Wilson & Harmon (1996, ApJ, 459, 288) with X-ray mesurements. The detected doubling, roughly at the periastron passage ($\phi_{\rm orb}$ = 0.997) of the neutron star, disappeared in about 40 days ($\phi_{\rm orb}$ = 0.377), which is hard to be explained in the case that the origin of these lines should be around the Be star.

Acknowledgements. We are pleased to thank those colleagues who gave permission for publishing some of their figures, which rendered this paper more suitable for a faster comprehension of the arguments discussed.

This research has made use of NASA's Astrophysics Data System.

References

Abdo, A.A., et al., 2009, ApJS, 183, 44
Abraham, J., et al., 2008, PhRL, 101, 1101
Alves, V.M., et al., 2003, Baltic Astron, 12, 33
Alves, V.M., et al., 2005, in *14th European Workshop on White Dwarfs*, D. Koester & S. Moehler (eds.), ASP Conf. Ser., 334, 561
Baade, W., & Zwicky, F., 1934, PhR, 45, 138
Bartko, H., 2007, talk at the Frascati Workshop on *Multifrequency Behaviour of High Energy Cosmic Sources*
Bartolini, C., et al., 1978, IAUC, 3167
Bednarek, W., et al., 1990, A&A, 236, 268
de Bernardis, P., et al., 2000, Nature, 404, 955
Blümer, J., Engel, R., & Hörandel, J.R., 2009, PrPNP, 63, 293
Boesgaard, A.M., 1984, AJ, 89, 1635
Bouvier, J., 1990, AJ, 99, 946
Bringmann, T, Bergström, L., and Edsjö, J. 2007, J. High Energy Phys., 01, 049
Burles, S., Nollet, K.M., & Turner, M.S., 2001, ApJ, 552, L1
Castro-Tirado, A.J., 2002, in *Multifrequency Behaviour of High Energy Cosmic Sources*, F. Giovannelli & L. Sabau-Graziati (eds.), Mem. S.A.It., 73, 337
Charpinet, S., et al., 1996, ApJ, 471, L103
Charpinet, S., et al., 2005a, 2005, A&A, 437, 575
Charpinet, S., et al., 2005b, A&A, 443, 251
Chartres, M., & Li, F., 1977, IAUC, 3154
Chaty, S., 1998, *PhD thesis*, University Paris XI
Chaty, S., 2007, in *Frontier Objects in Astrophysics and Particle Physics*, F. Giovannelli & G. Mannocchi (eds.), Italian Physical Society, Editrice Compositori, Bologna, Italy, 93, 329
Cheng, A.F. & Helfand, D.J., 1983, ApJ, 271, 271
Coburn, W., et al., 2002, ApJ, 580, 394
Colafrancesco, S., 2006, ChJA&AS, 6, 95
Colafrancesco, S., 2008, ChJA&AS, 8, 61
Colafrancesco, S., 2007, talk at the Frascati Workshop on *Multifrequency Behaviour of High Energy Cosmic Sources*
Colafrancesco, S., & Mele, B., 2001, ApJ, 562, 24
Colafrancesco, S., Profumo, S., & Ullio, P., 2006, A&A, 455, 21
Costa, E. *on behalf of the BeppoSAX GRB Team*, 1999, A&ASS, 138, 425
Costa, E., et al., 1997, astro–ph/9706065v1
Dar, A., 2006, in *Multifrequency Behaviour of High Energy Cosmic Sources*, F. Giovannelli & L. Sabau-Graziati (eds.), ChJA&A, 6 Suppl. 1, 323
Dar, A., De Rújula, A., 2004, Phys. Rep. 405, 203

De Angelis, A., Mansutti, O., & Persic, M., 2008, Il N. Cim., 31, No. 4, 187
Denegri, D., 2006, talk at the Vulcano Workshop on *Frontier Objects in Astrophysics and Particle Physics*
Dermer, C.D., et al., 2009, NJPh, 11, 1
De Roeck, A., 2008, NuPhS, 175–176, 493
Dolez, N., et al., 2006, A&A, 446, 237
Fargion, D., 2003a, in *Multifrequency Behaviour of High Energy Cosmic Sources*, F. Giovannelli & L. Sabau-Graziati (eds.), ChJA&A Suppl., 3, 472
Fargion, D.: 2003b, in *Frontier Objects in Astrophysics and Particle Physics*, F. Giovannelli & G. Mannocchi (eds.), Italian Physical Society, Editrice Compositori, Bologna, Italy, 85, 267.
Fargion, D., Grossi, M., 2006, in *Multifrequency Behaviour of High Energy Cosmic Sources*, F. Giovannelli & L. Sabau-Graziati (eds.), ChJA&A 6 Suppl. 1, 342
Feroci, M., 2001, in *Frontier Objects in Astrophysics and Particle Physics*, F. Giovannelli & G. Mannocchi (eds.), Italian Physical Society, Editrice Compositori, Bologna, Italy, 73, 287
Fierro, J.M., et al., 1993, ApJ, 413, L27
Finger, M.H., Wilson, R.B., & Harmon, B.A., 1996, ApJ, 459, 288
Forman, W., et al., 1978, ApJS, 38, 357
Frontera, F., 2003, ChJAS, 3, 439
Garcia-Alvarez, D., et al., 2003, A&A, 397, 285
Giacconi, R., et al., 1962, PhRL, 9, 439
Giangrande, A., et al., 1977, IAUC, 3129
Giangrande, A., et al., 1980, A&ASS, 40, 289
Giovannelli, F. (ed.), 1985, *Multifrequency Behaviour of Galactic Accreting Sources*, Editrice SIDEREA, Roma, Italy, p. 1–371.
Giovannelli, F., 1994, SSR, 69, 1
Giovannelli, F., 2005, *The Impact of Multifrequency Observations in High Energy Astrophysics*, PhD Thesis, University of Barcelona, Spain
Giovannelli, F., 2007, in *Frontier Objects in Astrophysics and Particle Physics*, F. Giovannelli & G. Mannocchi (eds.), Italian Physical Society, Editrice Compositori, Bologna, Italy, 93, 3
Giovannelli, F., et al., 1982, in *Proc. Second European IUE Conference*, E. Rolfe (ed.), ESA SP-157, 159
Giovannelli, F., et al., 1982, in *Proc. Third European IUE Conference*, E. Rolfe (ed.), ESA SP-176, 233
Giovannelli, F., et al., 1983, AcA, 33, 319
Giovannelli, F., et al., 1984, in *Proc. Fourth European IUE Conference*, E. Rolfe (ed.), ESA SP-218, 439
Giovannelli, F., et al., 1984, in *Proc. Fourth European IUE Conference*, E. Rolfe (ed.), ESA SP-218, 359
Giovannelli, F., et al., 1985, in *Multifrequency Behaviour of Galactic Accreting Sources*, F. Giovannelli (ed.), Edizioni Scientifiche SIDEREA, Roma, p. 284
Giovannelli, F., et al., 1986a, in *New Insight in Astrophysics, Proc. Joint NASA/SERC/ESA Conference*, E. Rolfe (ed.), ESA SP-263, 459
Giovannelli, F., et al., 1986b, IAUC 4284
Giovannelli, F., et al., 1987, IAUC 4368
Giovannelli, F., et al., 1987, Mem. SAIt., 58, 205
Giovannelli, F., et al., 1990a, ApSS, 169, 55
Giovannelli, F., et al., 1990b, ApSS, 169, 139
Giovannelli, F., & Ziółkowski, J., 1990, AcA, 40, 95
Giovannelli, F., et al., 1991, A&AS, 87, 89
Giovannelli, F., & Sabau-Graziati, L., 1992, SSR, 59, 1
Giovannelli, F., et al., 1995, A&AS, 114, 341
Giovannelli, F., & Sabau-Graziati, L., 2001, ApSS, 276, 67
Giovannelli, F., & Sabau-Graziati, L., 2004, SSR, 112, 1
Giovannelli, F., & Mannocchi, G. (eds.), 2007, *Frontier Objects in Astrophysics and Particle Physics*, Italian Physical Society, Editrice Compositori, Bologna, Italy, Vol. 93
Giovannelli, F., et al., 2007, A&A, 475, 651
Giovannelli, F., & Sabau-Graziati, L., 2008, ChJAS, 8, 1
Giovannelli, F., & Mannocchi, G. (eds.), 2009, *Frontier Objects in Astrophysics and Particle Physics*, Italian Physical Society, Editrice Compositori, Bologna, Italy, Vol. 98

GLAST Science Brochure (March 2001), http://glast.gsfc.nasa.gov/science
Guarnieri, A., et al., 1985, in *Multifrequency Behaviour of Galactic Accreting Sources*, F. Giovannelli (ed.), Edizioni Scientifiche SIDEREA, Roma, p. 310.
Hartle, J.B., Thorne, K.S., 1968, ApJ 153, 807
Hartman, R.C., et al., 1999, ApJS, 123, 79
Henry, R.C., 1999, ApJ, 516, L49
Henry, R.C.: 2002, in *Multifrequency Behaviour of High Energy Cosmic Sources*, F. Giovannelli & L. Sabau-Graziati (eds.), Mem. S.A.It., 73 N. 1, 67
Huang, S.-S., 1972, ApJ, 171, 549
Johnson, W. N., III, Harnden, F.R., Jr., & Haymes, R.C., 1972, ApJ, 172, L1
Joy, A.H., 1956, ApJ, 124, 317
Karakuła, S., & Tkaczyk, W., 1985, in *Multifrequency Behaviour of Galactic Accreting Sources*, F. Giovannelli (ed.), Editrice SIDEREA, Roma, Italy, p. 243
Kilkenny, D., et al., 1997, MNRAS, 285, 640
Kiplinger, A.L., 1979, AJ, 84, 655
Klebesadel, R.W., Strong, I.B., & Olson, R.A., 1973, ApJ, 182, L85
Lamzin, S.A., et al., 1996, A&A, 306, 877
Landolt, A.U., 1968, ApJ, 153, 151
Lena, P., 1988, *Observational Astrophysics*, Springer–Verlag Berlin–Heidelberg, Germany.
Leventhal, M., MacCallum, C.J., & Stang, P.D., 1978, ApJ, 225, L11
Li, F., et al., 1979, ApJ, 228, 893
Lichti, G.G., et al., 1994, in *Multi-wavelength continuum emission of AGN*, IAU Symposium No. 159, p. 327
Lichti, G.G., et al., 1995, A&A, 298, 711
Liller, W., 1975, IAUC 2780
de Loore, C., et al., 1984, A&A, 141, 279
Malesani, D., 2006, *PhD thesis*, SISSA/ISAS
Martinez-Pais, I.G., et al., 1994, A&A, 291, 455
de Martino, D., et al., 1989, in *The 23rd ESLAB Symposium on Two Topics in X Ray Astronomy. Volume 1: X Ray Binaries*, p. 519
Mather, J.C., et al., 1994, ApJ, 420, 439
Mattei, J.A., et al., 1985, *AAVSO Monograph*, Cambridge, MA (USA)
Mazets, E.P., & Golenetskii, S.V., 1988, Sov. Sci. Rev. E. Astrophys. Space Phys., 6, 283
Meištas, E.G. & Solheim, J.-E. (eds.), 1993, Baltic Astron., Vol. 2, No. 3-4, p. 357-571
Meszaros, P., & Rees, M.J., 1992, ApJ, 397, 570
Metcalfe, T.S., et al., 2005, A&A, 435, 649
Miyaji, T., Hasinger, G., & Schmidt, M., 2000, A&A, 353, 25
Morselli, A., 2007, talk at the European Conference on *High Energy Physics*
Murdin, P., 1975, IAUC, 2784
Nel, H.I., de Jager, O.C., 1994, in *The Second Compton Symposium*, C.E. Fichtel, N. Gehrels & J.P. Norris (eds.), *AIP Conf. Proc.* 304, 91.
Netterfield, C.B., et al., 2002, ApJ, 571, 604
Nicastro, L., et al., 2001, in *Gamma Ray Bursts in the Afterglow Era*, E. Costa, F. Frontera & J. Hjorth (eds.), Springer Verlag, Heidelberg, Germany, p. 198
Nitta, A., et al., 2009a, ApJ, 690, 560
Nitta, A., et al., 2009b, JPhCS, 172, 2073
Oreiro, R., et al., 2005, A&A, 438, 257
Orlandini, M, dal Fiume, D., 2001, in *X-Ray Astronomy: Stellar Endpoints, AGN, and the Diffuse X-Ray Background*, N.E. White, G. Malaguti & G.C. Palumbo (eds.), AIP Conf. Proc., 599, 283
Panagia, N., 2006, talk at the Vulcano Workshop on *Frontier Objects in Astrophysics and Particle Physics*
Paredes, J.M., 2006, talk at the Vulcano Workshop on *Frontier Objects in Astrophysics and Particle Physics*
Paredes, J. M., Bosch-Ramon, V.,& Romero, G. E., 2006, A&A, 451, 259
Patterson, J., Robinson, E.L., & Kiplinger, A.L., 1978, ApJ, 226, L137
Pian, E., & Hjorth, J., 2003, ChJAS, 3, 461
Piccioni, A., et al., 2000, A&A, 354, L13
Piran, T., 1999a, in *Gamma Ray Bursts: The First Three Minutes*, J. Poutanen & R. Svensson (eds.), ASP Conf. Ser., 190, 3
Piran, T.: 1999b, Phys. Rep., 314, 575
Piran, T., 2000, Phys. Rep., 333, 529
Plagemann, S.P., 1969, Communications of the Konkoly Observatory, No. 65 (Vol. VI, 1), p. 21
Priedhorsky, W.C., & Terrell, J., 1983, Nature 303, 681

Ressel, M.T., & Turner, M.S., 1990, Comments Astrophys., 14, 323
Robinson, E.L., 1976, ARA&A, 14, 119
Robinson, E.L., & McGraw, J.T., 1976, ApJ, 207, L37
Rosenberg, F.D., et al., 1975, Nature, 256, 628
Santangelo, A., 2008, talk at the Vulcano Workshop on *Frontier Objects in Astrophysics and Particle Physics*
Smak, J., 1969, AcA, 19, 155
Smak, J., 1981, AcA, 31, 395
Soderblom, D.R., 1976, IAUC, 2971
Sokolsky, P.V., 2006, JPhCS, 47, 260
Solheim, J.-E., 1993, Baltic Astron., 2, 363
Solheim, J.-E., 2003, Baltic Astron., 12, 463
Spillantini, P., 2007, in *Frontier Objects in Astrophysics and Particle Physics*, F. Giovannelli & G. Mannocchi, (eds.), Italian Physical Society, Editrice Compositori, Bologna, Italy, 93, 53
Srianand, R., Petitjean, P., & Ledoux, C., 2000, Nature, 408, 931
Stanev, T., 2007a, NuPhS, 165, 3
Stanev, T., 2007b, NuPhS, 168, 252
Stanev, T., 2007c, astro-ph 07112282
Stover, R.J., et al., 1980, ApJ, 240, 597
Streitmatter, R.E., 2005, talk at the Aspen Workshop on *Physics at the end of galactic cosmic ray spectrum*
Swanenburg, B.N., et al., 1981, ApJ, 243, L69
Winget, D.E., Nather, R.E., & Hill, J.A., 1987, ApJ, 316, 305
Winget, D.E., et al., 2004, ApJ, 602, 109
Wood, K.S., et al., 1984, ApJS, 56, 507
Ziółkowski, J., 2007, in *Frontier Objects in Astrophysics and Particle Physics*, F. Giovannelli & G. Mannocchi (eds.), Italian Physical Society, Editrice Compositori, Bologna, Italy, 93, 713